広島大学学位請求論文

Contribution of oxidative DNA damages to bactericidal effects caused by pulsed discharge with water-cavitation

（水中パルス放電の殺菌効果における DNA 酸化損傷の寄与）

２０１６年

工藤　健一

（岡山大学自然生命科学研究支援センター）

目次

主論文

Contribution of oxidative DNA damages to bactericidal effects caused by pulsed discharge with water-cavitation

Ken-ichi Kudo

2016

Contents

General Introduction

1. Application of plasma techniques

In recent years, interest for discharge plasma is increased as a method of solving some environmental and medical problems. It has been found that the plasma causes various active components such as physical shockwaves, high-electric field, reactive oxygen species (ROS) and ultraviolet light (UV) [Sato et al., 1996; Sun et al., 1997, 1999; Miichi et al., 2002; Yasuoka and Sato, 2009]. The utilization of plasma and its products described above have been utilized as methods for the clarification of industrial wastewater contaminated by various microorganisms and the decomposition of recalcitrant organic compounds, as well as medical procedures such as cancer therapy and disposal equipment sterilization [Jiang et al., 2014; Moreau, 2008; Preis et al., 2013]. Plasma is a partially or fully ionized gas consisting of electrons, ions, and neutrals, and has the characteristics of electrical neutrality and high conductivity. When voltage is applied between a pair of electrodes in an underwater reactor, initially electrons in the electric field receive several electron volts (eV) of energy, and are accelerated in the electric field (equivalent to electron temperature of $>10^4$ K). Then, these energetic electrons excite the atoms and molecules presenting between the electrodes, thereafter leading to the formation of plasma [Jiang et al., 2014; Sato, 2009; Sun et al., 1997]. The plasma generation causes the physical shockwaves accompanying the expansion of volume against liquid phase, the luminescence containing UV, and reactive chemical species containing ROS [Jiang et al., 2014; Sun et al., 1997]. Since the plasma generation needs huge amount of electricity in water, gas

bubbling assistance has been used for these discharge systems [Bai et al., 2010; Miichi et al., 2002; Shih and Locke, 2009]. However, the large-scale bubbling assistance system is less efficiently. Therefore, I adopt here an alternative method to reduce used electricity.

2. Generating mechanism of ROS by underwater plasma

Electrons accelerated by an applied electric field excite water and oxygen molecules between the electrodes, resulting in forming ROS, such as hydroxyl (OH) radical, ozone (O_3), singlet oxygen ($^1O_2$), and hydrogen peroxide (H_2O_2). After plasma generation by the discharge, OH radical, atomic hydrogen (H), and atomic oxygen (O), have been characteristically recognized by the distinct emission signatures, including the 309 nm-wavelength-peak derived from the $A^2\Sigma^+$-to-$X^2\Pi$ transition of OH radical, part of the Balmer series from H, and the 777 nm-wavelength-peak from O [Miichi et al., 2002; Sato et al., 1996; Sun et al., 1997]. The luminescences are emitted through the recombination of such chemical species, leading to the formation of relative stable species, such as molecular hydrogen, water molecule (H_2O) and H_2O_2 [Sun et al., 1997; Jiang et al., 2014]. These reactions seem to be generated on the boundary between plasma and water of the bubble [Jiang et al., 2014; Miichi et al., 2002; Shih and Locke, 2009]. H_2O_2 generated in water by plasma seems to play an important role in a mechanism of the bactericidal effect [Sato et al., 1996], which is formed via the recombination of two OH radicals each other [Gupta and Bluhm, 2007; Sato et al., 1996]. Thus, the importance of

ROS has been recently recognized for sterilization effect caused by the plasma, and some previous studies have quantitatively determined the yield of ROS formed via plasma by colorimetry with indicator chemicals, such as terephthalic acid [Bai et al., 2010; Sahni and Locke, 2006; Sato et al., 1996]. I discuss here what kinds of ROS contribute to the sterilization mechanism and which cellular parts are their biological targets.

3. The bactericidal effect and oxidative DNA damages caused by underwater plasma

The bactericidal effects of underwater electrical discharge are reported for *Saccharomyces cerevisiae*, *Staphylococcus aureus*, *Escherichia coli*, and *Bacillus subtilis* [Chen et al., 2008; Kadowaki et al., 2009, Sato et al., 1996]. A previous study indicated that the irreversible breakdown of cell membrane in the presence of a high-electric field contributes to the sterilizing mechanism [Sale and Hamilton, 1967]. Recently, ROS has been recognized as an important factor mediating the bactericidal action. Some investigations for plasma treatment of organic substances have already suggested that OH radical plays the most important role in their degradations [Miichi et al., 2002; Sahni and Locke, 2006]. However, it has been unclear which of the plasma actions are key factors and which targets in cell are important for its bactericidal effect. One study has shown the possibility that ROS formed by plasma sterilize ballast seawater with its generated OH radical [Bai et al., 2010]. Also, H_2O_2 as well as OH radical

formed by underwater electrical discharge are thought to be involved in the mechanism for sterilization [Sato et al., 1996]. Meanwhile, DNA damage in bacterial cells induced by hybrid gas-liquid electrical discharge was investigated by the denaturing gradient gel electrophoretic analysis [Chen et al., 2008]. This study discusses that such DNA damage is more important for sterilizing effect, which may be caused by UV and/or H_2O_2 generated by plasma. Also, water-surface plasma accompanying molecular oxygen (O_2) gas flow causes DNA degradation in *B. subtilis* cells [Kadowaki et al., 2009]. This study suggests that OH radical and O_3 attack cellular DNA and/or membrane as the biological targets in the plasma-induced sterilization. However, these studies used different methods for discharge each other as problems, disturbing further analysis for the sterilization mechanism of underwater plasma. Among all types of cellular damage, DNA damage is thought to be the most critical for cell viability. For example, ionizing radiation produces a large amount of ROS, which oxidize biological materials in the irradiated living organism. Such damaging pathway via ROS is well known as “indirect effect,” which is the predominant route of radiation damage. Fenton reaction is another method of oxidizing DNA in many previous studies [Rivière et al., 2006; Walling, 1975]. H_2O_2 shows electrically neutrality [Test and Weiss, 1984; Weiss, 1982], and therefore it can penetrate through cell membrane. Thus, H_2O_2 produces OH radical by its reduction reaction with metal ions such as iron ion in cell [Walling, 1975]. It is one of reasons of H_2O_2 damaging ability, although it has slow reactivity to organic substrates. Alternatively, H_2O_2

can be also degraded into OH radicals by luminescence such as UVB, which is also generated by the plasma [Sato, 2009]. Synergistic bactericidal effects of H_2O_2 and UV have been reported [Hartman and Eisenstark, 1978].

4. Survey of this thesis

For this theme, I consider that the plasma causes the bactericidal effect via ROS, which generate oxidative damage to biological target, such as cellular DNA.

In Chapter 1, I expose plasmid DNA by the plasma to determine the amount of DNA strand breaks and oxidized base lesions in the DNA molecules. In this experiment, pulsed discharge with cavitation was used to generate plasma in the water. I used X-rays as the control in this study. After detection of oxidative DNA damage caused by plasma, I also treated *E. coli* cells with the plasma and evaluated the cell survival and chromosomal DNA damage. From these experimental results, I conclude that the plasma causes oxidative DNA damage, which is one of the pathways contributing to the bactericidal action.

In Chapter 2, I further elucidate the underlying mechanism of bactericidal effect of the plasma. I evaluated the quantitative yields of ROS such as OH radical and H_2O_2, induced by the pulsed discharge. Then, I analyzed DNA damage including double strand break (DSB) and oxidative base lesions in *E. coli* cells treated by the plasma. My present result indicates that the plasma-treated cells showed a distinct sensitivity for the

pulsed discharge, and harbored oxidative DNA damage. I also quantitatively measure oxidative base lesions, such as 8-hydroxyguanine (8-OH-G) and 5-hydroxycytosine (5-OH-C), induced in *E. coli* cells after the plasma treatment. From the experimental result, I conclude that the bactericidal effect of plasma caused by the pulsed discharge is mediated via ROS, and the magnitude of the effect is dependent on the yields of oxidative DNA damage.

Chapter 1

Quantitative analysis of oxidative DNA damage induced by high-voltage pulsed discharge with cavitation

Summary

Pulsed discharge is used for sterilization and disinfection, but the details of the molecular mechanisms remain largely unknown. Since pulsed discharge generates ROS, I analyzed the oxidative DNA damages after pulsed discharge treatment to consider the involvement of ROS in the damaging process. I applied pulsed discharge with cavitation to plasmid DNA molecules and estimated the yields of the damages by agarose gel electrophoresis. The treated DNA contained various oxidative DNA damages, including single and double strand breaks and base lesions. The yields of the damages increased in response to the energy used for the pulsed discharge. I also measured the yield of 8-OH-G, one of the major oxidative base lesions, in the treated plasmid DNA by mass spectrometry quantitatively and found that the yield of the oxidative base lesion corresponded to the increment of the applied energy. In addition, I observed the involvement of *mutM* gene, which is responsible for repair of 8-OH-G, in the increased sensitivity of *E. coli* cells to the pulsed discharge. Therefore, ROS seem to mediate the sterilization ability of the pulsed discharge.

1. Introduction

In recent years, interest for pulsed discharge is increased as a method of solving some problems in liquid system. Particularly, sterilization and detoxification of industrial wastewater contaminated by microorganisms and hazardous substances are the most widely anticipated ones among the promising uses of pulsed discharge [Moreau, 2008; Preis et al., 2013]. In fact, the application for sterilization has been also attempted from early period of the history [Hamilton and Sale, 1967]. These efforts have continued in the recent years, and there are some reports on sterilization using pulsed discharge in the water phase contaminated with various microorganisms, including *S. cerevisiae*, *E. coli*, and *B. subtilis* [Chen et al., 2008; Kadowaki et al., 2009; Sato et al., 1996]. Although pulsed discharge shows such effective sterilization ability, little is known about the molecular mechanism underlying this sterilization.

High voltage generates plasma in water [Sato et al, 1996; Sun et al., 1999]. In the plasma, physical and electrical shocks seem to be important for degradation of target substances [Benz and Zimmermann, 1980; Chen et al., 2008; Sato et al., 1996]. In particular, plasma also generates luminescence, such as UV, and ROS, both of which can damage biological constructs. Previous studies indicate that pulsed discharge generates various species of ROS such as OH radical, $^1O_2$, O, O_3, and H_2O_2 in water [Miichi et al., 2002; Sato et al., 1996; Sun et al., 1997, 1999; Yasuoka and Sato, 2009]. Endogenously and exogenously generated ROS are known to consistently damage most biological components, including DNA, resulting

in aging and carcinogenesis. Therefore, oxidative damages of DNA are considered the most important causative mechanism in the many biological disorders that result from the use of pulsed discharge. Indeed, chromosomal DNA damage was observed in *B. subtilis* cells treated with pulsed discharge [Kadowaki et al., 2009]. Additionally, argon gas discharge produced oxidative DNA bases such as thymine glycol (TG), 2,6-diamino-4-hydroxy-5-formamidopyrimidine (Fapy-G), 4,6-diamino-5-formamidopyrimide (Fapy-A), and 8-hydroxyadenine in solution, indicating the involvement of ROS [Su et al., 2011]. Thus, I suppose that pulsed discharge causes damage to living organisms through oxidative DNA damages. However, little quantitative information is available about the oxidative DNA damage induced by pulsed discharge.

In this study, I conducted a quantitative analysis of oxidative DNA damage induced by pulsed discharge in water using circular plasmid DNA. After processing by pulsed discharge, appropriate DNA glycosylases uncover the correspondent oxidative base lesions in the damaged DNA. Mass spectrometry (MS) measurements of the treated DNA molecules showed the production of 8-OH-G, a major oxidative DNA base lesion. The yields of the DNA damages increased in proportion to the processing time of pulsed discharge. Here, I employed cavitation with pulsed discharge, because cavitation can reduce the discharge onset voltage to generate plasma without supplying additional gases [Ihara, 2011]. However, cavitation itself showed limited abilities for sterilization and ROS generating [Jyoti and Pandit, 2001; Soyama and Muraoka, 2010]. Therefore,

I also evaluated the ability of cavitation to generate oxidative DNA damage for definition of the pulsed discharge abilities on this system. In this study, I used X-rays for the control experiments, which are well known to cause oxidative DNA damage through ROS generation. I found some differences in the DNA damage caused by pulsed discharge and that caused by ionizing radiation. Finally, I treated *E. coli* cells with pulsed discharge coupled with cavitation and evaluated cell survival and chromosomal DNA damage. From these results, I conclude that pulsed discharge causes oxidative DNA damage, one of the pathways contributing to sterilization.

2. Materials and methods

2.1. Materials

pUC19 plasmid DNA (2686 base pairs) was prepared from *E. coli* HB101 harboring the DNA using the QIAGEN Plasmid Mega Kit (Qiagen, Netherlands). For the experiments, I used only good-quality DNA aliquots consisting of >95% of supercoiled form. Agarose S for gel electrophoresis was purchased from Nippon Gene (Japan). *E. coli* endonuclease III (Endo III) and formamidopyrimidine DNA glycosylase (Fpg) were prepared as reported previously [Asagoshi et al., 2000a, 2000b]. Calf intestine alkaline phosphatase was purchased from Toyobo (Japan). $^{15}N_5$-labeled 8-hydroxy-2′-deoxyguanosine ($^{15}N_5$-8-OH-dG) was obtained from Cambridge Isotope Laboratories (United States). Other chemicals and enzymes were from Wako Pure Chemicals Industries (Japan), unless otherwise stated. The bacterial strain for preparing the DNA was a laboratory stock.

2.2. Treatments for causing DNA damage

2.2.1. Pulsed discharge with cavitation

The experimental system for pulsed discharge with cavitation consisted of a plasma reactor and power supply for plasma generation, and a water circulation apparatus consisting in water tank and pump (Fig. 1-1a). The inverter power supply provided both positive and negative voltages to the plasma reactor, which had the power supply frequency of 10 kHz. The reactor had a nozzle with an inner diameter of 3 mm for the generation of

water-cavitation, and both high-voltage– and grounded-electrodes for the plasma induction (Fig. 1-1b). The pulsed voltage and current were measured by a 1:1000 high-voltage probe (Tektronix, United States) and a current probe (Pearson Electronics, United States), respectively. Both waveforms were monitored by a digital oscilloscope (LeCroy, United States). Typical waveforms are shown in Fig. 1-2. Averaged discharge power (P) for 10 periods was calculated with the following formula:

$$P = \frac{1}{10T}\int_0^{10T} V(t)\cdot I(t)dt$$

where $V(t)$, $I(t)$, and T indicate pulsed voltage, pulsed current, and cycle of $V(t)$, respectively. Applied energy, which indicates the energy inputted to the total solution, was calculated for 2 dm^3 of solution as follows;

$$E = \frac{P \times \tau}{v}$$

where E, τ, and v indicate applied energy, treatment time, and solution volume, respectively. The electric strengths at the center between electrodes and in the vicinity of respective electrodes were estimated to be 2.5 kV cm^{-1} and 6 kV cm^{-1} respectively, upon application of 1 kV across the electrodes distance 4 mm in the electric field under an ideal condition. For cavitation condition of this apparatus, calculated cavitation number (σ) is 0.088 on the basis of the previous study [Gogate and Pandit, 2004]. The maximum water pressure in circuit was 1.1 × 10^6 kg m^{-1} s^{-2} at top of the nozzle orifice.

Aqueous DNA solution (2 dm^3; 5 mg dm^{-3}) was circulated for 2 min

at a flow rate of 4.6 dm^3 min^{-1} for mixing, before pulsed discharge treatment. Then, the DNA solution was treated by pulsed discharge with cavitation in water circulation at a flow rate of 20 dm^3 min^{-1}. The pulsed discharge was applied in the discharge gap located between the two electrodes. The treated solution was sampled every 12 s up to 96 s. All pulsed discharge experiments were performed at room temperature.

2.2.2. X-irradiation

Aqueous DNA solution (1 cm^3; 5 mg dm^{-3}) was irradiated with X-rays in a microtube. The irradiation was carried out using an X-ray generator (HW-150R, HITEX, Japan) operating at 150 kVp and 8 mA without any filters at room temperature. The absorbed dose rate was 15.2 Gy min^{-1}, measured with the RAMTEC Smart Dosimeter (TOYO Medic, Japan).

2.3. DNA damage analyses

2.3.1. Nicking assay for damaged plasmid DNA

After treatment with the pulsed discharge or X-rays, 100 ng of plasmid DNA was digested by 40 ng of Endo III or Fpg in 10 mM Tris (amino-2-hydroxymethyl-1,3-propandiol-hydrochloride)-HCl buffer, pH 7.5, containing 1 mM ethylenediamine tetraacetic acid (EDTA), and 100 mM sodium chloride (NaCl) at 37°C for 60 min. The enzyme reaction was halted by adding the gel loading solution [0.25% (w/v) bromophenol blue, 30% (v/v) glycerol, and 10 mM EDTA]. The digested DNA (20 ng) was

analyzed by gel electrophoresis on a 1.2% (w/v) agarose gel in TAE buffer (40 mM Tris, 40 mM acetic acid, and 1 mM EDTA) containing 0.8 μg dm^{-3} of ethidium bromide (EtBr). The run condition was 50 V for 105 min (gel size: 50 × 60 mm) [Terato et al., 2008]. The electrophoresed gel image was captured with an AE-6933FXCF charged-coupled device camera system (ATTO, Japan) equipped with a UV trans-illuminator. The data from the captured images were analyzed using the ImageJ software (National Institute of Health, United States) [Rasband, 2012]. Since EtBr has lower affinity for the supercoiled form of circular plasmid DNA than for both the open circular and linear forms, the intensity of the band corresponding to the supercoiled form was corrected using a factor of 1.4 [Gulston et al., 2002].

2.3.2. Measurement of 8-OH-dG

2.3.2.1. Sample Preparation

To measure 8-OH-dG, 500 ng of plasmid DNA was hydrolyzed with 0.6 U of nuclease P1 at 37°C for 30 min to obtain digestion to the nucleotide components in 0.1 cm^3 of solution. The reaction mixture was hydrolyzed with 1.2 U of alkaline phosphatase in 10 mM Tris-HCl, pH 8.5, at 37°C for 30 min to form the nucleosides. For liquid chromatography-tandem MS (LC-MS/MS) analysis, 0.01 cm^3 of $^{15}N_5$-8-OH-dG solution (0.1 mg dm^{-3}) was added to the sample as the internal standard after incubation. Before analysis, the respective samples were purified through a Nanosep Centrifugal Device with Omega

membrane (Pall, United States).

2.3.2.2. Liquid chromatography-tandem mass spectrometry (LC-MS/MS)

LC-MS/MS was performed using a Shimadzu LCMS-8030 triple quadrupole mass spectrometer with an electro-spray ionization (ESI) probe. The LC system consisted of a DGU-14 AM degasser, an LC-30AD pump, a CTO-10Avp column oven, and a SIL-30AC autosampler. LC was separated on a KINETEX 1.7-μm C18 column (ϕ 2.1 mm × 100 mm: Phenomenex, United States) at 40°C. The mobile phase, consisting of 0.1% (v/v) aqueous formic acid and acetonitrile, was used in a linear gradient from 2% to 40% acetonitrile (the increasing rate was 50% min^{-1}). The flow rate was 0.2 cm^3 min^{-1} and the injection volume was 2.0 × 10^{-2} cm^3. MS operating parameters were as follows: probe voltage, 4.5 kV; desolvation line temperature, 250°C; block heater temperature, 400°C; drying gas flow, 15.0 dm^3 min^{-1}; nebulizing gas flow, 1.5 dm^3 min^{-1}. ESI was in the positive ion mode. MS data acquisition was performed in the multiple reaction monitoring (MRM) mode. For 8-OH-dG, the collision energy was optimized at 16 eV, and the MRM transition was from 284.00 to 168.10 m/z, corresponding to the $[M + H]^+$ precursor and product ions, respectively. For $^{15}N_5$-8-OH-dG, the collision energy was optimized at 14 eV, and the MRM transition was from 289.00 to 173.05 m/z, corresponding to the $[M + H]^+$ precursor ion and product ion, respectively.

The calibration curve of 8-OH-dG was linear in the range of 1.8-180 pmol cm^{-3} (seven-point calibration, $|r^2| > 0.999$). The limit of

detection was determined to be 49.5 fmol cm^{-3} (signal-to-noise, S/N = 3), corresponding to about 1.0 fmol injected.

2.4. Analyses of bacterial viability and chromosomal DNA damage

E. coli KA796 (wild type) and NR11040 (Δ*mutM*) strains were laboratory stocks [Santos and Drake, 1994]. Both strains were cultured in LB medium (10 g dm^{-3} of tryptone, 5 g dm^{-3} of yeast extract, and 10 g dm^{-3} of NaCl) at 37°C with shaking (200 rpm) until OD_{600} reached 0.3. The grown cells were washed twice with phosphate buffered saline (PBS: 0.01 M phosphate, 0.138 M NaCl, and 2.7 mM potassium chloride, pH 7.4) and were resuspended into the same buffer. The cells (10^6 colony-forming units [CFU] per cubic centimeter) were treated by the pulsed discharge or X-rays in a similar way for the DNA as described in *Section 2.2*. After these treatments, the treated cell suspensions were 10-fold diluted in PBS, and the aliquot (0.1 cm^3) were seeded in triplicate to a 96-well flat-bottom polystyrene microplate. MTS solution [0.05 cm^3; 3-(4,5-dimethylthiazol-2-yl)-5-(3-carboxymethoxyphenyl)-2-(4-sulfopheny l)-2H-tetrazolium salt solution (Promega, United States) supplemented with tryptone (30 g dm^{-3}), yeast extract (15 g dm^{-3}), and glucose (1 g dm^{-3})] was added to each well. After incubation in the dark at 37°C for 7 h, the absorbance of each well at 490 nm was measured using a Wallac 1420 ARVO MX (PerkinElmer, United States) spectrophotometer. In this assay, cell viability is indicated by the formation of water-soluble formazan, which has a specific color, by the reduction of tetrazolium salts by the

dehydrogenases in viable cells in the presence of a carbon source [Kuda et al., 2004; Leverone et al., 1996].

Chromosomal DNA damage was analyzed with static field gel electrophoresis, as previously described [Nakano et al., 2007]. Briefly, after treatment with pulsed discharge, 9 cm^3 of the treated cell suspension was collected by centrifuge (2270 × *g*, 10 min). The cell pellet was resuspended in 0.025 cm^3 of PBS and mixed into 3-fold volume of molten SeaPlaque GTG agarose (Cambrex, United States). The molded agarose cell plugs were incubated in 2 cm^3 of lysis buffer consisting of 1% Sarkosyl, 50 mM Tris-HCl (pH 8.0), and 25 mM EDTA at 50°C for 16 h. After washing in 10 cm^3 of TE buffer, the each plug was inserted into 1% (w/v) agarose gel (length × width = 18 cm × 12 cm) and electrophoresed with 17 mA of constant current in 1× TBE buffer for 20 h. The electrophoresed gel image was analyzed as described in *Section 2.3.1*.

3. Results

3.1. Oxidative DNA damage by pulsed discharge

Plasmid DNA, which adopts a circular conformation when it is intact, is useful as a substrate for the study of DNA damage [Gulston et al., 2002; Terato et al., 2008]. The independent proliferative DNA molecule shows occurrence of DNA strand break when changing its conformation from intact supercoiled form (SC) to opened circular (OC) and linear (LN) forms. The OC form contains at least one single strand break (SSB) in one molecule of plasmid DNA, whereas the LN form includes one DSB in one molecule. Since these three different forms can be separated by agarose gel electrophoresis under appropriate conditions, I can observe the occurrence of DNA strand breaks in the substrate DNA molecules.

In this study, I subjected the pUC19 plasmid in aqueous solution to pulsed discharge with cavitation under circulation. The aliquots of treated DNA solution sampled in chronological order were analyzed by agarose gel electrophoresis to observe the damage (Fig. 1-3). Concurrently, I observed the corresponding yields induced by X-rays for comparison (Fig. 1-4). After treatment of pulsed discharge, the amount of intact SC DNA decreased with the experimental time, while the single-damaged OC DNA containing one SSB increased simultaneously (Figs. 1-3a and 1-3d). By further extending the experimental time, complex-damaged LN DNA carrying a DSB appeared. This could be due to the pulsed discharge, because the treatment time was proportional to the applied energy of pulsed discharge. The results without glycosylase treatment for damage detection

indicated that the strand breaks were clearly generated by the pulsed discharge. In addition, the fraction of SC exponentially decreased to almost zero at 400 mJ cm^{-3} applied energy. On the other hand, the LN fraction increased linearly as the applied energy increased throughout the treatment period. The DNA irradiated by X-rays showed similar conformational changes with increase in the treatment time (Figs. 1-4a and 1-4d). I estimated the yields of SSB and DSB from the results of the agarose electrophoreses. The decrement of the SC fraction was fitted with a least-mean-square formula [$y = ce^{-mx}$]. The yield of SSB was calculated from the slope m and the D_{37} value (dose when the fraction is 37%), which gives on average 1 SSB per plasmid molecule, with the Poisson distribution in the single hit model [Hall and Giaccia, 2012]. The yield of DSB was estimated from the slope of the initial increment of the LN fraction. The yield of SSB induced by the pulsed discharge was 27.9 pmol J^{-1} (Table 1-1), whereas the yield of SSB with X-rays was 560 pmol J^{-1}. Thus, the pulsed discharge was 20 times less efficient than X-rays in producing SSB. The yield of DSB with the pulsed discharge was 0.426 pmol J^{-1}. The ratio of SSB to DSB due to the pulsed discharge was 66:1. On the other hand, the yield of DSB with X-rays showed 6.36 pmol J^{-1} and the ratio of SSB to DSB was 88:1. Usually, the ratio of SSB and DSB is reported to be 50–100 times in ionizing radiation, showing that my present results can be considered reliable.

For detection of oxidative base lesions, I lysed the sample DNA with specific DNA glycosylases. Endo III added oxidative pyrimidine

lesions such as TG to the generated strand breaks (Figs. 1-3b and 1-3e). Similarly, Fpg piled up oxidative purine lesions including 8-OH-G (Figs. 1-3c and 1-3f). The increments of the damage induced by these DNA glycosylases indicate that the pulsed discharge generates oxidative base lesions. The increments in the SSB and DSB after treatment with the DNA glycosylases were regarded as isolated and clustered oxidative base lesions, respectively. Here, isolated lesion means that the damaging site is sparsely generated on the DNA and clustered lesion indicates closely spaced lesions within one or two helical turns of DNA [Hall and Giaccia, 2012]. In other words, the respective sensitive sites for those enzymes included directly generated strand breaks and the corresponding oxidative base lesions. Therefore, I calculated the yields of the isolated and clustered base lesions from the yields of the respective enzyme sensitive sites after subtracting the SSB and DSB generated by the pulsed discharge, respectively. The yields of isolated and clustered oxidative pyrimidine damages with the pulsed discharge were 12.6 and 0.226 pmol J^{-1}, respectively (Fig. 1-5). Likewise, the yields of isolated and clustered oxidative purine damages were 55.5 and 0.594 pmol J^{-1}, respectively (Fig. 1-5). The yields of the respective damages induced by X-rays and the pulsed discharge were almost similar for the proportion (Fig. 1-4). Though, the yields with the pulsed discharge were 13–74 times lower than those with X-rays (Table 1-1 and Fig. 1-5). Both results suggest that the pulsed discharge and ionizing radiation damage DNA in a similar manner, but the two forces show different efficiency for damaging.

3.2. Contribution of cavitation in oxidative damage caused by pulsed discharge

Cavitation facilitates the formation of plasma without supplying additional gases [Ihara, 2011], and I used cavitation to generate plasma in my system. However, ROS might be generated through the collapse of microbubbles produced by cavitation itself [Soyama and Muraoka, 2010]. Therefore, I evaluated the generation of DNA damage in cavitation without pulsed discharge. With cavitation only, the SC fraction decreased to 80% of the original value after treatment for 10 min (Figs. 1-6a and 1-6d). This decrease corresponded to the increment of the OC fraction entirely, while no LN fraction was detected. The respective yields of SSB and isolated oxidative pyrimidine and purine damages induced by cavitation alone were 0.946, 5.39, and 19.1 pmol s^{-1}, respectively. They were 50–300 times less than the yields of the damages obtained with the pulsed discharge. At the same time, with cavitation treatment alone, I did not detect any clustered DNA damages such as DSB and clustered oxidative pyrimidines. Only oxidative purine damages at 4.57×10^{-4} pmol s^{-1} were detected, a concentration much less than that obtained with the pulsed discharge. Thus, the oxidative DNA damages were derived mainly from pulsed discharge, and cavitation played a minor role in generating the damages in this system.

3.3. Quantitative estimation of 8-OH-dG induced by pulsed discharge

The electrophoretic analysis of plasmid DNA treated by the pulsed

discharge revealed the generation of 8-OH-G as Fpg-sensitive sites. Here, the treated DNA was subjected to MS for a more quantitative analysis of the yield of 8-OH-dG. During the LC separation, 8-OH-dG appeared 2.31 min after injection. $^{15}N_5$-8-OH-dG, in which the five nitrogen atoms were isotopically labeled with the stable ^{15}N, was used as the standard material for the quantitative analysis. The typical separation data are shown in Fig. 1-7a. The amount of 8-OH-dG in the DNA treated by the pulsed discharge increased in response to the applied energy (Fig. 1-7b). The increment of the damage followed a quadratic curve. Thus, the increasing rate was reduced in the high-dose region, similar to what was observed with X-rays (the inset of Fig. 1-7b). According to the initial slope of the growing curves, the yield of 8-OH-dG was estimated to be about 360 and 290 pmol J^{-1} for the pulsed discharge and X-rays, respectively. So, the yields of the pulsed discharge and X-rays were similar. On the other hand, the yields of the Fpg-sensitive sites in the electrophoretic analyses were different between the pulsed discharge and X-rays (Table 1-1).

3.4. Viability and DNA damage in E. coli cells treated with pulsed discharge

Up to this point, I observed that the pulsed discharge generated oxidative damages in DNA substrates. Especially, I showed that the yield of 8-OH-G quantitatively depended on the applied energy of pulsed discharge by MS analysis. Therefore, I then investigated the contribution of the *mutM* gene to the cellular sensitivity to the pulsed discharge using *E. coli* strains

lacking that gene. *mutM* is the structural gene for Fpg, the specific DNA glycosylase removing 8-OH-G from DNA [Michaels et al., 1991; Tajiri et al., 1995; Tchou et al., 1991]. I exposed wild-type *E. coli* cells and mutant strains lacking *mutM* to the pulsed discharge and estimated the cellular sensitivities by MTS assay, which determines cellular viability through measuring energy metabolism (Fig. 1-8). After treatment with pulsed discharge coupled with cavitation, *E. coli* NR11040 strain lacking *mutM* was more sensitive than KA796, the wild type strain containing this gene (Fig. 1-8). The sensitivity of the mutant was 10 times that of the wild type after treatment for 90 s. Since Fpg is an enzyme responsible for repairing 8-OH-G, this result confirms the previous results with DNA substrates. At the same time, I analyzed the chromosomal DNA damage induced by the pulsed discharge in *E. coli* cells. As the exposure time progressed, DNA fragmentation increased (Fig. 1-9). The band released from the original gel plug position on the electrophoresed gel consisted of damaged DNA, i.e., DSB were generated. Since both cellular sensitivity and DNA damage increased simultaneously, DNA damage seems to be one of the mechanisms responsible for the bactericidal effects. The presence of the *mutM* gene had no significant influence on the amount of DNA damage, because there was no time to process damaged DNA by Fpg in this experiment.

4. Discussion

The pulsed discharge has the ability to sterilize wastewater, and its capability is now expanding. In this study, I elucidated the mechanism through which the pulsed discharge kills target microorganisms, and my results will be useful for developing an effective application procedure. Since some previous reports indicated that the pulsed discharge generates various kinds of ROS, I assumed that oxidative damages are involved in its mechanism. Among all types of cellular damage, DNA damage is thought to be the most critical in terms of cell survival. After treatment with the pulsed discharge, oxidative DNA damages including SSB, DSB, and oxidative base lesions such as 8-OH-G were detected by electrophoretic analysis (Fig. 1-3). The yields of these damages increased with the treatment time. Thus, the generation of DNA damage corresponded to the applied energy of pulsed discharge. The DNA irradiated by X-rays showed similar response to the absorbed dose, i.e., the applied energy (Fig. 1-4). Ionizing radiation produces large amount of ROS, which damage biological materials oxidatively in the irradiated living organism. Such damages via ROS are well known as “indirect effects,” which are the predominant route of radiation damage, and are abundant after exposure to ionizing radiations. My electrophoresis assay for plasmid DNA molecules indicated that the yields of the isolated and clustered DNA damages after treatment with the pulsed discharge were approximately 20 and 50 times lower, on average, than those with X-rays, respectively (Table 1-1 and Fig. 1-5). A possible reason for this result could be the different transmission efficiency of

energy between the pulsed discharge and X-rays. Namely, X-rays transduce the energy for target materials as absorbed energy efficiently, while it is unclear how much of the energy from the pulsed discharge is used for ROS generation. An indirect study indicated that the efficiency of OH radical generation, which was measured as the yield of 2-hydroxyterephthalic acid as the oxidative product of terephthalic acid, in gas-liquid electrical discharge was 0.39 nmol J^{-1} ($G_{OH} = 3.74 \times 10^{-3}$) [Sahni and Locke, 2006]. On the other hand, the yields of ROS from X (γ)-rays were well investigated. For example, a study indicated that the yield of OH radical was 0.28 μmol J^{-1} ($G_{OH} = 2.7$) [Appleby and Schwarz, 1969]. Thus, the yields of DNA damages with the pulsed discharge and X-rays might differ according to their ROS generation efficiencies.

On the other hand, I indicated here that the generation ratios of each DNA lesion were similar (Table 1-1 and Fig. 1-5). The total yields of isolated and clustered oxidative DNA damages with the pulsed discharge were 95.7 and 1.25 pmol J^{-1}, respectively, whose ratio was 77:1 (Table 1-1 and Fig. 1-5). Likewise, the total yield of isolated and clustered oxidative DNA damages with X-rays were 1730 and 62.9 pmol J^{-1}, respectively, whose ratio was 28:1. Thus, the proportion of clustered damage in total DNA lesions with the pulsed discharge is 2–3 times lower than that for X-rays, suggesting that X-rays generate clustered damage in DNA more effectively than the pulsed discharge does. Additionally, the proportions of oxidative pyrimidine and purine damages with the pulsed discharge are 13% and 58% in isolated damage and 18% and 48% in clustered damage

(Table 1-1 and Fig. 1-5), respectively. Likewise, those for X-rays are 26% and 42% in isolated damage and 27% and 63% in clustered damage. Thus, the relative ratios of the yields of the base lesions generated by the pulsed discharge are different from those generated by X-rays.

I also found a difference in the proportion of the yields of enzyme-sensitive sites to strand breaks between the pulsed discharge and X-rays (Fig. 1-10). The number of isolated Endo III- and Fpg-sensitive sites was 1.5 and 3 times the number of SSB in DNA damages caused by the pulsed discharge, respectively. These ratios were similar to those obtained with X-rays. On the other hand, the numbers of clustered enzyme-sensitive sites were different between the pulsed discharge and X-rays. The number of clustered Endo III- and Fpg-sensitive sites was 1.5 and 2.4 times the number of DSB in damages caused by the pulsed discharge, respectively. Thus, the pulsed discharge generated Endo III- and Fpg-sensitive sites with similar ratios between isolated and clustered species. Contrarily, the numbers of clustered Endo III- and Fpg-sensitive sites were 3.6 and 7.2 times higher than the number of DSB in damages caused by X-rays, respectively. Thus, the pulsed discharge generates clustered damage in DNA less efficiently than X-rays do. Ionizing radiation passes through the target material as a beam and generates ROS along the track. OH radical, the most hazardous ROS, can travel a very short distance because it is highly reactive [Roots and Osada, 1975]. Thus, DNA damages caused by ionizing radiation can be localized close to the beam track; therefore, ionizing radiations such as X-rays generate clustered DNA

damages more effectively than other oxidative damaging agents do. On the other hand, the pulsed discharge seems to disperse the damages because the electric current gives rise to plasma, in which ROS will be generated diffusely.

Additionally, I should consider the differences in the detectable objects between electrophoresis and mass spectrometry. I used Fpg for detecting the damages in electrophoresis analysis. Although the DNA glycosylase activity of Fpg shows broad substrate specificity, ranging from 8-OH-G [Boiteux et al., 1990; Tchou et al., 1991] to imidazole ring-opened substrates such as Fapy-G [Haraguchi and Greenberg, 2001; Wiederholt et al., 2003] and Fapy-A [Boiteux et al., 1992], the specificity toward 8-OH-G is twice that toward the ring-opened substrates. Moreover, Fpg can incise the DNA strands at AP sites owing to its AP lyase activity [Chetsanga and Lindahl, 1979; O'Connor and Laval, 1989]. AP sites are known to be one of the major lesions in gamma-irradiated DNA *in vitro*, which amount to approximately 40% of the total isolated damages [Ali et al., 2004; Terato et al., 2008]. Thus, the oxidative purine lesions obtained by electrophoretic analysis included various damages such as 8-OH-G, Fapy-G, and AP sites, which were excised by Fpg. The concentration of oxidative purine lesions, calculated from the increment of the LN fraction upon Fpg treatment, in the DNA solution treated by the pulsed discharge was approximately 570 pmol cm^{-3} (Fig. 1-3f). MS analysis revealed about 125 pmol cm^{-3} 8-OH-dG in the same treated sample (Fig. 1-7b). Thus, experimental methods using Fpg detect many kinds of oxidative guanine lesions including 8-OH-G, and the

higher yield of oxidative purines by electrophoresis was shown than the yield of 8-OH-G obtained by MS without other purine damages. This also indicates that the pulsed discharge generates 8-OH-G preferentially from among all other oxidative guanine lesions unlike ionizing radiations such as X-rays. Ionizing radiations generate Fapy-G in a yield greater than or equal to 8-OH-G [Chetsanga et al., 1981; Pouget et al., 2002]. The MS analysis results indicated almost similar yields of 8-OH-G with both the pulsed discharge and X-rays (Table 1-1 and Fig. 1-7). Contrarily, electrophoretic results with Fpg showed lower detectable amounts of oxidative purine damages with the pulsed discharge than those with X-rays. Therefore, the proportion of 8-OH-G in total purine lesions from the pulsed discharge was higher than that of X-rays. This means that X-rays produced a wide variety of purine damages, but the pulsed discharge preferentially made 8-OH-G. I need further study for elucidation of this difference.

As stated above, the pulsed discharge generates ROS and causes oxidative damage in target DNA. I also showed that *E. coli* cells lacking the *mutM* gene became sensitive to the pulsed discharge (Fig. 1-8). Because *mutM* encodes Fpg, which is a specific DNA glycosylase that removes oxidative guanine lesions from DNA, this result indicates that oxidative DNA damage is involved in the cytotoxicity of the pulsed discharge. The cellular viability of the wild-type strain treated with the pulsed discharge correlated with the corresponding yield of the LN fraction in the plasmid assay (Fig. 1-3d). Its correlation coefficient was estimated to be $|r| = 0.975$. This finding also supports that DNA strand break is involved in the killing

of *E. coli* cells. Here, it should be noted that most of the ROS generated by the pulsed discharge were outside the cells. Considering the amount of DNA damages obtained, I need to assume some mechanism for either the intracellular generation and/or the migration of ROS into the cells. The majority of ROS do not enter the cells through the cell membrane. Thus, extracellularly generated ROS are not likely to attack DNA in cells. One hypothesis for the origin of intracellular ROS is that the modification of the cell membrane by pulsed voltage, known as electroporation, leads to increased cell permeability and facilitates ROS passing through the cell membrane [Dev et al., 2000]. Another hypothesis is the involvement of some kinds of ROS that can pass through the cell membrane. As the major candidate, H_2O_2 is electrically neutral and has slow reactivity to organic substrates [Test and Weiss, 1984; Weiss, 1982]. It was previously reported that the pulsed discharge generated H_2O_2 [Sato et al., 1996]. That report also indicated that the increment in H_2O_2 levels was synchronized with the decrease in cell viability. H_2O_2 itself shows very low reactivity, but it can produce OH radicals by its reduction reaction with metal ions such as iron, termed the Fenton reaction [Walling, 1975]. Cells are rich in such metal ions, which are naturally involved in various normal metabolic reactions and can also generate OH radicals. Alternatively, H_2O_2 might be degraded into OH radicals in UV-treated cells. The pulsed discharge can generate UV, whose peak is at 309 nm due to the $A^2\Sigma^+$-to-$X^2\Pi$ (v = 0, 0) transition of OH radical [Sato et al., 1996; Sun et al., 1997; Yasuoka and Sato, 2009]. In this pathway, H_2O_2 generated outside cells moves into the cells, where UV

generated by the pulsed discharge transforms H_2O_2 into OH radicals through a photochemical reaction.

Furthermore, lipoperoxidation of cell membrane is thought to be another possible factor to damage DNA oxidatively via long-lived lipid peroxides [Yukawa and Nakazawa, 1980]. Among various ROS, $^1O_2$ is also generated by pulsed discharge [Sun et al., 1997, 1999; Yasuoka and Sato, 2009]. $^1O_2$ is known to be involved in the peroxidation process [O'Brien and Little, 1969], and $^1O_2$ can pass through the cell membrane similarly to H_2O_2 [Gorman et al., 1976]. Thus, $^1O_2$ might be an important factor for DNA damage with the pulsed discharge. In conclusion, the DNA damage in cells treated by the pulsed discharge are thought to be mainly caused by intracellular OH radicals, which could be due to multiple factors such as the increment of permeability and the dissociation of H_2O_2 via Fenton reaction and/or UV.

Figures and Table

Table 1-1 Strand breaks in the pUC19 plasmid DNA treated with the pulsed discharge or irradiated with X-rays.

	Pulsed Discharge		X-ray	
	Isolated damage (pmol J^{-1})	Clustered damage (pmol J^{-1})	Isolated damage (pmol J^{-1})	Clustered damage (pmol J^{-1})
Strand Break	27.9 ± 5.8	0.426 ± 0.090	560 ± 113	6.36 ± 4.56
Endo III sensitive site	40.5 ± 8.0	0.652 ± 0.115	1010 ± 180	23.2 ± 1.5
Fpg sensitive site	83.4 ± 31.8	1.02 ± 0.21	1280 ± 200	46.1 ± 8.3

The values represent the mean of three experiments with their standard deviations (SD).

(a)

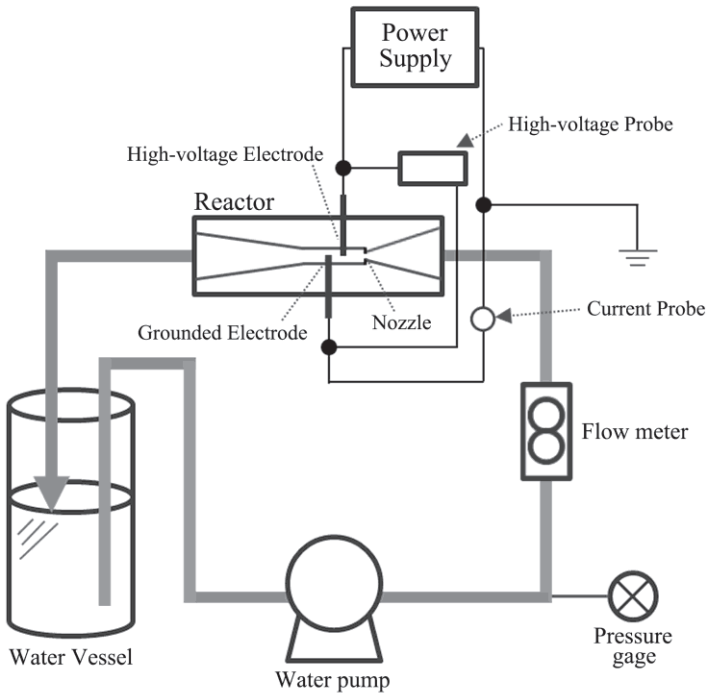
Power Supply
High-voltage Probe
High-voltage Electrode
Reactor
Current Probe
Grounded Electrode
Nozzle
Flow meter
Water Vessel
Water pump
Pressure gage

(b)

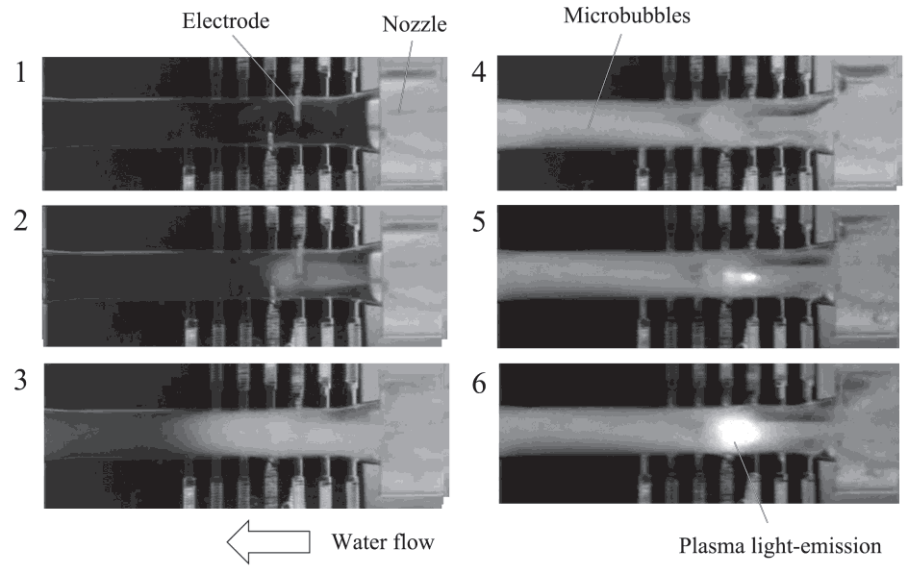
Electrode
Nozzle
Microbubbles
1
2
3
4
5
6
Water flow
Plasma light-emission

Figure 1-1. Apparatus for generating pulsed discharge with cavitation. (a) Schematic diagram of the apparatus. The reactor is an acrylic venturi tube equipped with two electrodes for discharge and a 3 mm-diameter nozzle for producing water-cavitation. The high-voltage electrode is set at a distance of 13 mm from the nozzle. The grounded electrode is 4 mm away from the other electrode. The electrodes are constituted by a stainless steel needle (SUS316) having a diameter of 1 mm and a length of 40 mm. The treatment volume of this apparatus is 2 dm^3.

(b) Continuous picture of the reactor from static condition to generation of plasma (Photos 1 to 6). Photo 1 indicates static condition with neither flow nor electric voltage. Photos 2-4 show water-cavitation occurrence in the reactor with 20 L min^{-1} water flow, and stable microbubble generation is observed in Photo 4. Then, the light-emission from plasma channel is observed in the limited distance between electrodes with voltage applying in Photos 5 and 6. Photo 6 represents maximum intensity of emission.

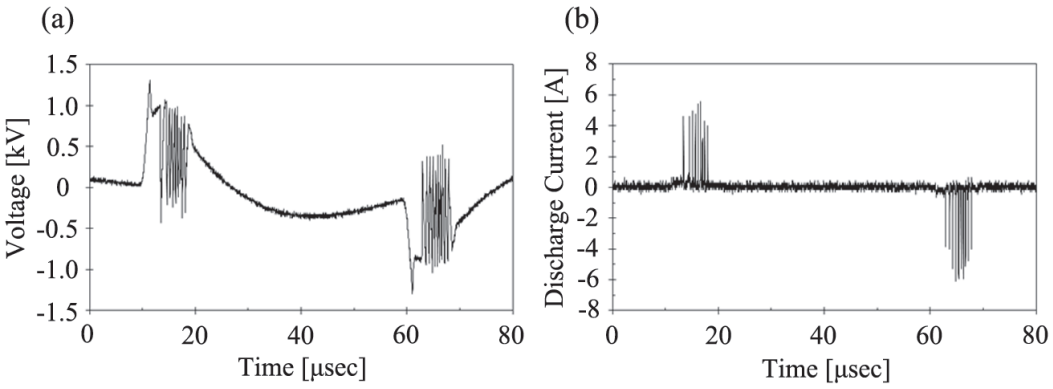

Figure 1-2. Typical waveforms of applied voltages (left panel) and discharge currents (right panel) are shown during discharge of the power supply at a frequency of 10 kHz.

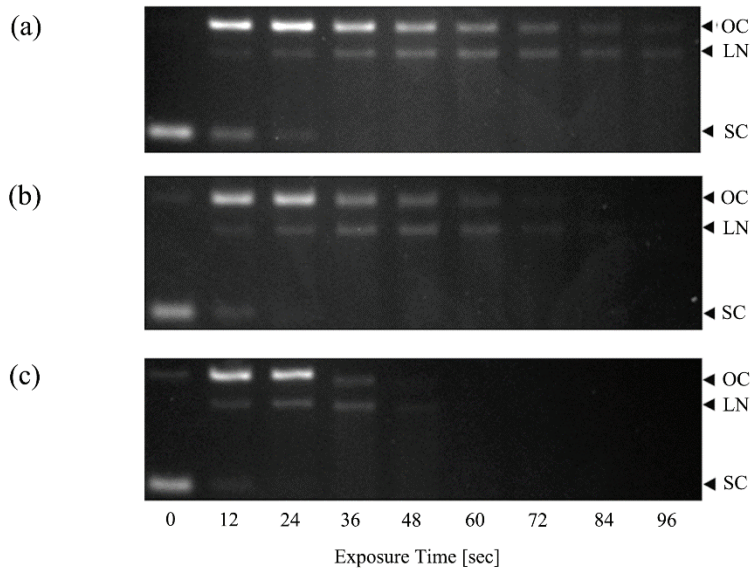
(a)
(b)
(c)
OC
LN
SC
0
12
24
36
48
60
72
84
96
Exposure Time [sec]

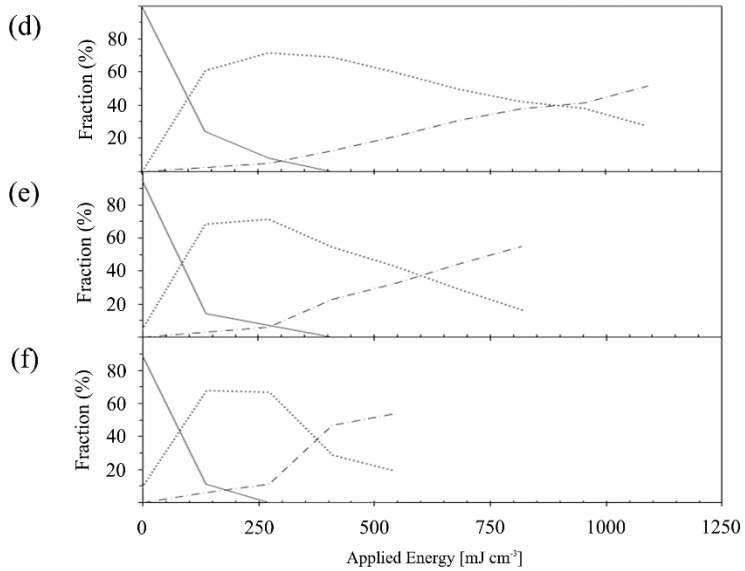
(d)
(e)
(f)
Fraction (%)
20
40
60
80
0
250
500
750
1000
1250
Applied Energy [mJ cm-3]

Figure 1-3. Agarose gel electrophoresis of pUC19 plasmid DNA treated with pulsed discharge with cavitation. (a–c) Electrophoretic profiles. The intact supercoiled DNA (SC) are damaged and converted first into open circular (OC) and then into linear form (LN). (d–f) Plots of the yields of the bands corresponding to those in (a–c). The solid, dotted, and broken lines represent SC, OC, and LN, respectively. (a, d) Control (in the absence of any enzyme); (b, e) Endo III treatment; (c, f) Fpg treatment. The applied energies were calculated from the resulting discharge power and exposure time. In this experiment, the average discharge power was approximately 23 W.

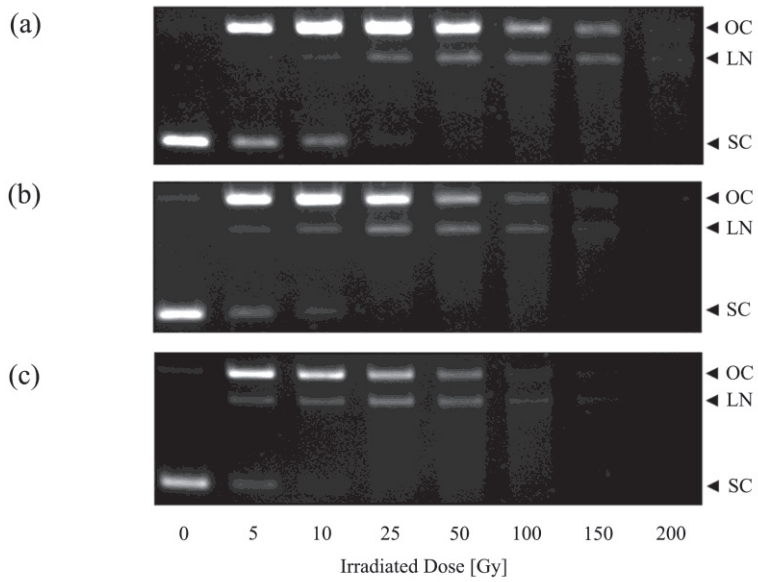
(a)
(b)
(c)
OC
LN
SC
0
5
10
25
50
100
150
200
Irradiated Dose [Gy]

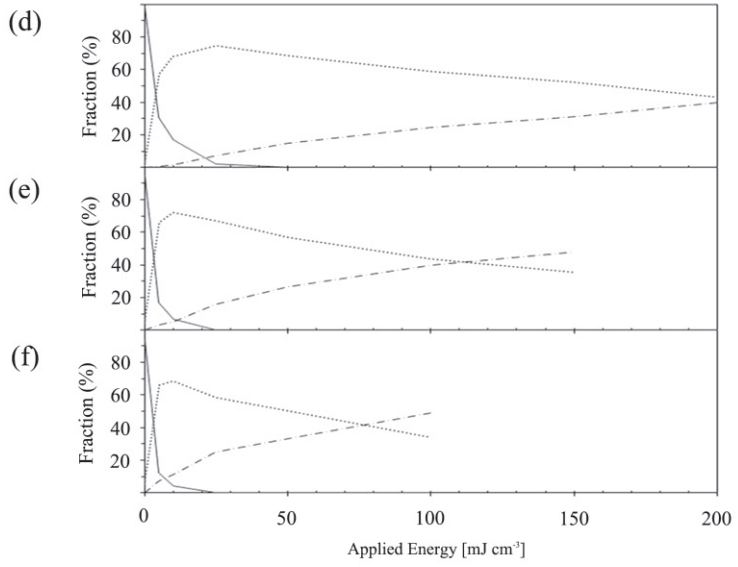
(d)
(e)
(f)
Fraction (%)
80
60
40
20
0
50
100
150
200
Applied Energy [mJ cm-3]

Figure 1-4. Agarose gel electrophoresis of pUC19 plasmid DNA irradiated with X-rays. (a–c) Electrophoretic profiles. The intact supercoiled DNA (SC) is damaged and converted first into open circular (OC) and then linear form (LN). (d–f) Plots of the yields of the bands corresponding to those in (a–c). The solid, dotted, and broken lines represent SC, OC, and LN, respectively. (a, d) Control (in the absence of any enzyme); (b, e) Endo III treatment; (c, f) Fpg treatment. The applied energies are calculated from the absorbed dose assuming that water density is $\rho = 1.0$ g cm^{-3}.

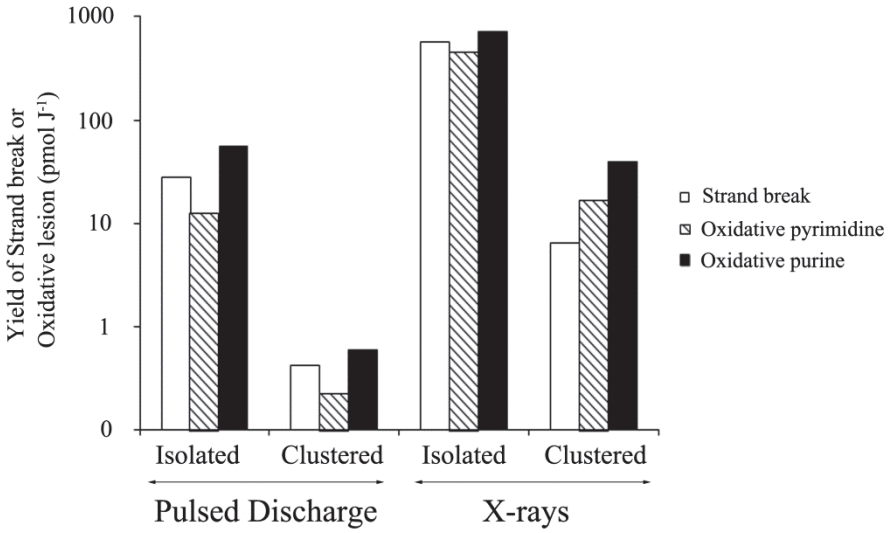

Figure 1-5. Calculated yields of oxidative pyrimidine (striped bar) and purine (closed bar) lesions induced by the pulsed discharge and X-ray from the electrophoretic analyses (Figs. 1-3 and 1-4). The respective yields are obtained by subtracting the amount of strand breaks (open bar) from the Endo III- and Fpg-sensitive sites shown in Table 1-1. Oxidative pyrimidine and purine lesions in isolation (Isolated) and in cluster (Clustered) are presented separately.

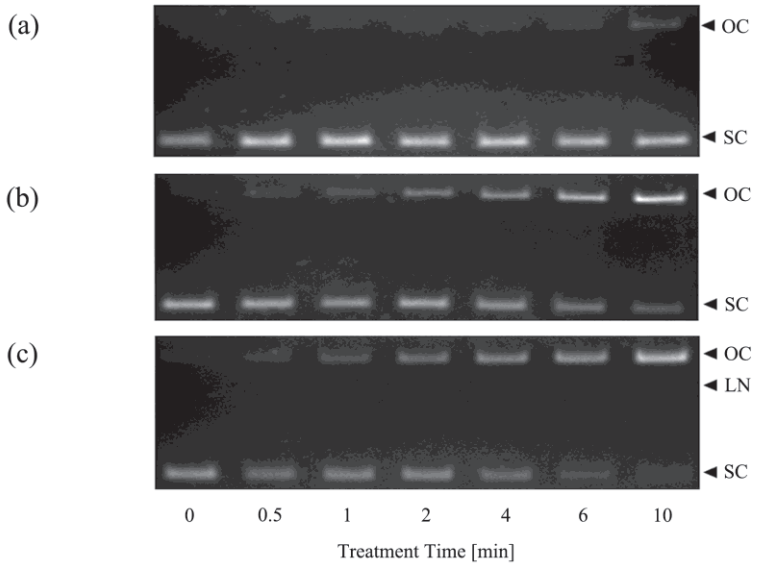
(a)
OC
SC
(b)
OC
SC
(c)
OC
LN
SC
0
0.5
1
2
4
6
10
Treatment Time [min]

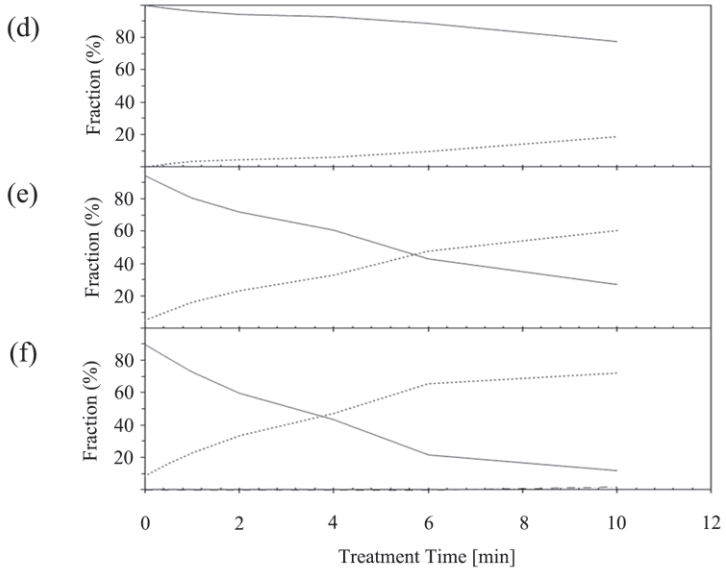
(d)
Fraction (%)
80
60
40
20
(e)
Fraction (%)
80
60
40
20
(f)
Fraction (%)
80
60
40
20
0
2
4
6
8
10
12
Treatment Time [min]

Figure 1-6. Agarose gel electrophoresis of pUC19 plasmid DNA treated only with cavitation in the absence of pulse discharge. (a–c) Electrophoretic profiles. The intact supercoiled DNA (SC) is damaged and converted first into open circular (OC) and then linear form (LN). (d–f) Plots of the yields of the bands corresponding to those in (a–c). The solid, dotted, and broken lines represent SC, OC, and LN, respectively. (a, d) Control (in the absence of any enzyme); (b, e) Endo III treatment; (c, f) Fpg treatment.

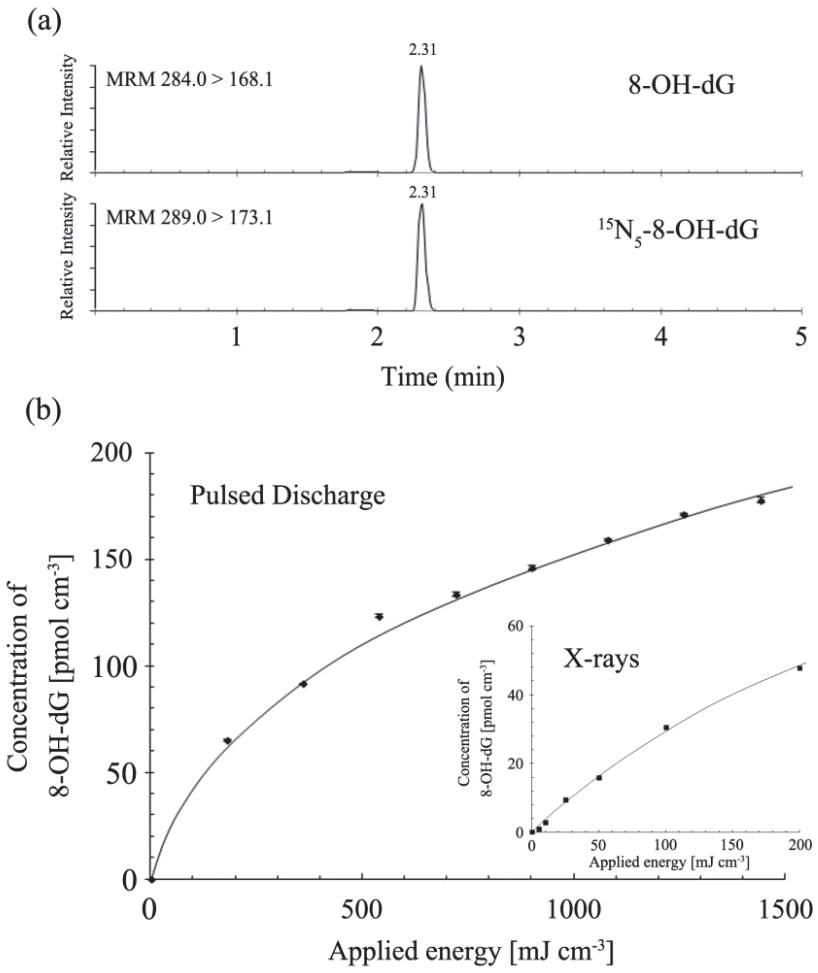

Figure 1-7. (a) LC-MS/MS chromatograms of 8-OH-dG derived from pUC19 plasmid DNA treated with the pulsed discharge for 96 s (top) and $^{15}N_5$-8-OH-dG as the internal standard (bottom) in the multiple reaction monitoring mode. (b) Yields of 8-OH-dG in the treated DNA as a function of the energy of the pulsed discharge and X-rays (inset) determined by LC-MS/MS. The results represent the mean of three experiments with their SD. In this experiment, the average discharge power was approximately 30 W.

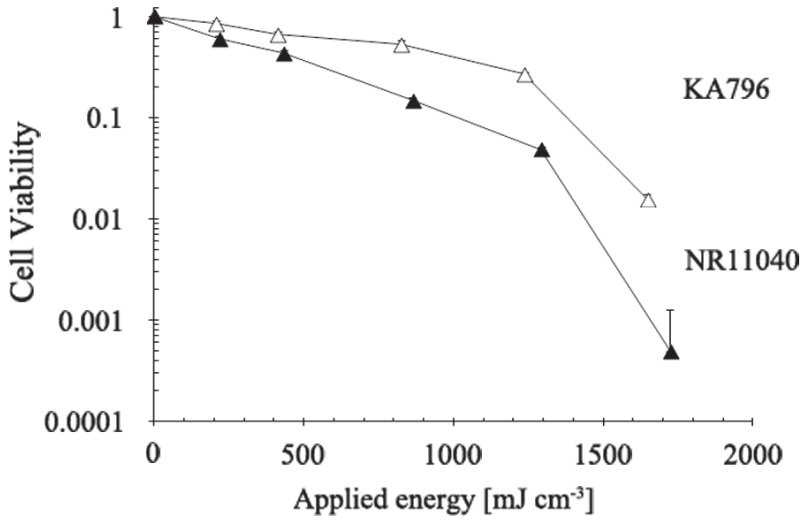

Figure 1-8. Viability of *E. coli* KA793 (wild-type, open triangle) and NR11040 (*mutM* gene mutation, closed triangle) cells treated with the pulsed discharge in deionized water. Cell viability determined by a colorimetric assay using MTS is almost equivalent to the survival fraction. Data represent the SD of three experiments. The average discharge power is equivalent to approximately 35 W.

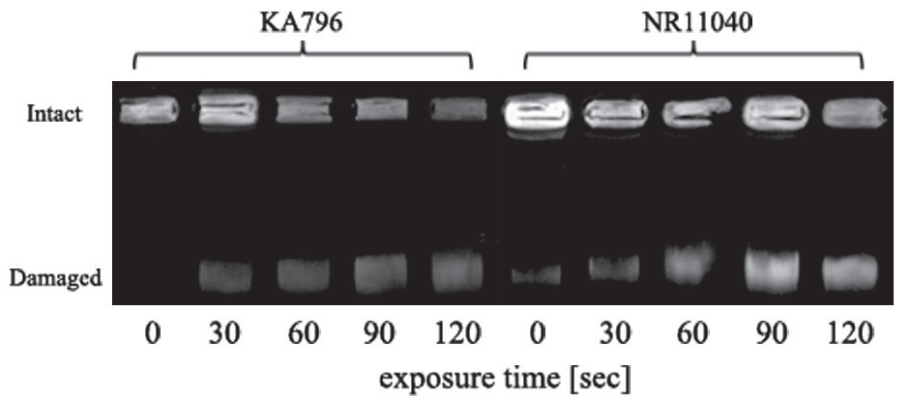

Figure 1-9. Agarose gel electrophoresis of the DNA of *E. coli* KA793 and NR11040.

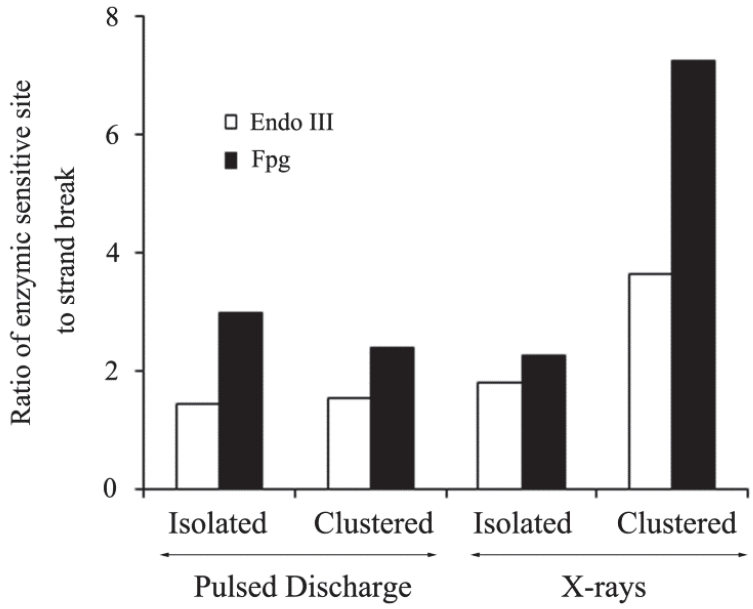

Figure 1-10. Ratios of enzyme-sensitive sites to strand break obtained with the pulsed discharge and X-rays. The ratio of Endo III- (open bar) and Fpg- (closed bar) sensitive sites are shown separately. These ratios were calculated from the data of the electrophoretic analyses (Figs. 1-3 and 1-4) summarized in Table 1-1.

Chapter 2

Oxidative DNA damage caused by pulsed discharge with cavitation on the bactericidal function

Summary

Plasma-based techniques are expected to have practical use for wastewater purification with a potential for killing contaminated microorganisms and degrading recalcitrant materials. In the present study, I analyzed oxidative DNA damage in bacterial cells treated by the plasma to unveil its mechanisms in the bactericidal process. *E. coli* cell suspension was exposed to the plasma induced by applying an alternating-current voltage of about 1 kV with bubbling formed by water-cavitation, termed pulsed discharge with cavitation. Chromosomal DNA damage, such as DSB and oxidative base lesions, increased proportionally with the applied energy, as determined by electrophoretic and mass spectrometric analyses. Among the base lesions identified, the yields of 8-OH-G and 5-OH-C in chromosomal DNA increased by up to 4- and 15-fold, respectively, compared to untreated samples. The progeny DNA sequences, derived from plasmid DNA exposed to the plasma, indicated that the production rate of 5-OH-C exceeded that of 8-OH-G, as G:C to A:T transitions accounted for 65% of all base changes, but only a few G:C to T:A transversions were observed. The cell viabilities of *E. coli* cells decreased in direct proportion to increases in the applied energy. Therefore, the plasma-induced bactericidal mechanism appears to relate to oxidative damage caused to bacterial DNA. These results were confirmed by observing the generation of OH radicals and H_2O_2 molecules following the plasma exposure. I also compared my results with the plasma to those obtained with ^{137}Cs γ-rays, as a well-known

ROS generator to confirm the DNA-damaging mechanism involved.

1. Introduction

In recent years, the practical application of underwater electrical discharge has been anticipated as a strategic solution for clarifying industrial wastewater contaminated by various microorganisms and decomposing recalcitrant organic compounds [Jiang et al., 2014; Sato, 2009; Sun et al., 1997]. It has been shown that underwater electrical discharge causes bactericidal effect against *S. cerevisiae*, *S. aureus*, *E. coli*, and *B. subtilis* [Chen et al., 2008; Kadowaki et al., 2009; Sato et al., 1996]. When voltage is initially applied between a pair of electrodes in an underwater reactor to cause an electrical discharge, electrons are accelerated in the electric field, imparting to them the energy of several eV [Jiang et al., 2014; Sun et al., 1997]. These energetic electrons excite atoms and molecules presenting between the electrodes, thereafter leading to the formation of the plasma, an ionized gas consisting of ions and free electrons [Sato, 2009]. The plasma generates various active components such as ROS and UV [Jiang et al., 2014; Sato, 2009]. The generation of chemically active species in plasma can be recognized by distinct emission signatures, including the 309 nm-wavelength peak derived from the $A^2\Sigma^+$-to-$X^2\Pi$ (v = 0, 0) transition of the OH radical, part of the Balmer series from H, and the 777 nm-wavelength peak from O [Miichi et al., 2002; Sato et al., 1996; Sun et al., 1997]. Some previous studies with indicator chemicals showed that underwater electrical discharge generates such as OH radical and H_2O_2 [Sahni and Locke, 2006; Sato et al., 1996; Shih and Locke, 2009]. UV emitted from plasma typically consists of UVB,

derived from mainly OH radical, as well as UVC [Sun et al., 1997]. Additionally, bacterial cells are also exposed to the high-electric field applied to between electrodes in underwater electrical discharge. Among the potential bactericidal factors, it has been unclear which of those are key factors and which targets in cell are important for the bactericidal effect. A previous study indicated that the irreversible breakdown of cell membrane in the presence of a high-electric field contributes to sterilizing mechanism for microorganisms [Sale and Hamilton, 1967]. Recently, ROS has been recognized as an important factor mediating bacterial sterilization [Chen et al., 2008; Kadowaki et al., 2009; Sato et al., 1996]. Some investigations for plasma treatment of organic substances suggested that OH radical plays the most important role in the degradation of recalcitrant materials [Miichi et al., 2002; Sahni and Locke, 2006]. Plasma seemed to sterilize ship ballast water with its generated OH radical [Bai et al., 2010]. Also, OH radical and H_2O_2 formed by pulsed high-voltage discharge are thought to be involved in the mechanism for sterilization [Sato et al., 1996]. DNA damage in bacterial cells induced by hybrid gas-liquid electrical discharge was investigated by the denaturing gradient gel electrophoretic analysis [Chen et al., 2008]. Also, water-surface plasma accompanying O_2 gas flow was found to cause DNA degradation in *B. subtilis* cells [Kadowaki et al., 2009]. These studies may give us an involvement of oxidative DNA damage in the bactericidal ability.

Based on previous knowledge regarding the sterilizing mechanism of plasma, I reported that pulsed discharge with cavitation caused oxidative

DNA damage in treated plasmid DNA (Chapter 1). The pulsed discharge generates plasma in bubbling gases formed by water-cavitation, which is able to reduce the discharge onset voltage in contrast to direct water discharge system. The pulsed discharge caused DSB, which is difficult to be recovered by the most of DNA repair pathways, thus leading to lethal effects to cells (Chapter 1). DNA appears to be the most critical target affecting cell survival, and ROS generation following the plasma exposure will contribute to sterilization through oxidative DNA damage. I need to seek direct evidence for the involvement of ROS and related target(s) mediating the bactericidal effect of the pulsed discharge to elucidate the underlying molecular mechanism(s) involved.

In this study, I first evaluated the quantitative yields of OH radical and H_2O_2 induced by the pulsed discharge. Then, I analyzed DNA damage, such as DSB and oxidative base lesions, caused in *E. coli* cells after the plasma treatment. I also investigated the survival of treated cells. My present results indicated that treated cells showed a distinct sensitivity for the pulsed discharge and that they harbored oxidative DNA damage. These effects increased with increased pulsed discharge treatment time, and ROS yields increased in parallel. Therefore, I conclude that the bactericidal effect of pulsed discharge with cavitation is mediated via plasma-induced ROS.

2. Materials and methods

2.1. Materials

E. coli KA796 strain was an my laboratory stock [Santos and Drake, 1994]. *E. coli* JM109 competent cell used for gene transformations was obtained from Takara Bio Inc. (Japan). pUC19 plasmid was prepared from *E. coli* HB101 cells with the QIAGEN Plasmid Mega Kit (Qiagen, Netherlands) as described in Chapter 1. Pulse field gel certified agarose (Bio-Rad, United States) was used for static field gel electrophoresis (SFGE) experiments. 5-hydroxy-2′-deoxycytidine (5-OH-dC) was purchased from Carbosynth (United Kingdom). 8-OH-dG was from Wako Pure Chemicals Industries (Japan). $^{15}N_5$-labeled 8-hydroxy-2′-deoxyguanosine (L-8-OH-dG) and $^{13}C,^{15}N_2$-labeled 5-hydroxy-2′-deoxycytidine (L-5-OH-dC) were obtained from Cambridge Isotope Laboratories (United States) and Toronto Research Chemicals, Inc. (Canada), respectively. Disodium terephthalate (NaTA) was from Tokyo Chemical Industry Co., Ltd. (Japan). 2-hydroxyterephthalic acid (HTA) from Santa Cruz Biotechnology (United States) and *N*-ethyl-*N*-(2-hydroxy-3-sulfopropyl)-*m*-toluidine (TOOS) from Dojindo (Japan) were used for OH radical and H_2O_2 estimations. Unless otherwise stated, all other chemicals and enzymes were described in Chapter 1.

2.2. Treatment of pulsed discharge with cavitation

An experimental system for producing pulsed discharge with cavitation consisted of a plasma reactor and a power supply for discharge

generation and a water-circulation apparatus containing a water tank and pump, as described in Chapter 1 (Fig. 1-1a). An alternating-current voltage of 10 kHz frequency was provided by the inverter power supply to the plasma reactor. Typical waveforms of the applied voltages and discharge currents are shown in Fig. 2-1a.

The emission spectrum from the plasma measured by TM-UV/VIS Minispecrometer (C10082CA; Hamamatsu Photonics, Japan) is shown in Fig. 2-2; the peaks at 309 nm from OH radical, 656 nm from H_α, 486 nm from H_β, and 777 nm from O are observed. This spectrum indicates plasma generation in this apparatus.

E. coli cells were cultured in LB medium, and then resuspended in PBS after washed twice, as described in Section 2-4 of Chapter 1. This cell suspension (10^7 colony-forming units [cfu] per cubic centimeter) was diluted 25 fold in distilled water prior to the plasma exposure. Two dm^3 of bacterial suspension was first circulated for 2 min at a flow rate of 4.6 dm^3 min^{-1} to ensure the bacteria were well mixed before initiating the plasma treatments. Next, the suspension circulated at a flow rate of 20 dm^3 min^{-1} and then was treated by the plasma from 0 to 96 seconds.

Cell viabilities were measured by using a MTS (Promega, United States), which shows a specifically color due to the formation of formazan by the dehydrogenases in viable cells [Kuda et al., 2004]. The treated cell suspensions were 10-fold diluted in PBS, and the triple-partitioning aliquots (0.1 cm^3) were seeded to a 96-well flat-bottom polystyrene microplate. MTS solution [0.05 cm^3; MTS supplemented with tryptone (30

g dm^{-3}), yeast extract (15 g dm^{-3}), and glucose (1 g dm^{-3})] was added to each well. After incubation in the dark at 37°C for 7 h, the absorbance of each well at 490 nm was measured using a Wallac 1420 ARVO MX spectrophotometer (PerkinElmer, United States). pUC19 plasmid DNA were treated with the pulsed discharge, as described in Chapter 1.

2.3. γ-irradiation

E. coli cells and pUC19 plasmid DNA were irradiated in a microtube and a conical tube, respectively, with ^{137}Cs γ-rays (Gammacell 40, Atomic Energy of Canada, Canada) at room temperature. The average dose rate was 0.72 Gy min^{-1}. The irradiated samples were analyzed in the same way as the pulsed discharge, respectively.

2.4. Determination of ROS formations

OH radical yield was estimated by the fluorescence of HTA, derived from NaTA conversion [Armstrong et al., 1963]. Aqueous NaTA solution (0.5 mM) was treated by the pulsed discharge at the treatment times of 0, 12, 24, 48, and 96 s as described in *Section 2.2*. HTA formation was quantitated by reading emission at 425 nm (excitation at 315 nm) on an FP-750 spectrofluorometer (JASCO, Japan). A calibration curve for OH radical estimation was made from 0.1–20 nmol cm^{-3} of HTA (eight-point calibration, $|r^2| = 0.997$). H_2O_2 yield was determined by a colorimetric assay using an aqueous solution containing 1 mM 4-amino antipyrine, 1 mM TOOS, and 1 U cm^{-3} horseradish peroxidase [Tamaoku et al., 1982]. 0.1

cm^3 of the water treated by the pulsed discharge was added to 96-well microplates in triplicate, and 0.1 cm^3 of reagent solution was added to each well. After incubation at 37°C for 10 min in the dark, the absorbance at 560 nm was measured for H_2O_2 quantification with a Wallac 1420 ARVO MX spectrophotometer. H_2O_2 standards in the calibration curve ranged between 1–200 nmol cm^{-3} (eight-point calibration, $|r^2| > 0.999$). The yields of OH radical and H_2O_2 following exposure to γ-rays were determined as described above for the pulsed discharge experiments.

2.5. DNA damage analyses

2.5.1. SFGE experiments

Chromosomal DNA damage in *E. coli* cells were analyzed by SFGE, as described in Chapter 1. The cell solution was treated by the pulsed discharge at the treatment times of 24, 48, 72, and 96 sec as described in *Section 2.2*. Briefly, treated cells (10^8 cfu cm^{-3}) were collected by centrifugation (3000 × *g*, 10 min, 4°C) and then embedded into agarose gel plugs (10^6 cfu per plug). Plugs were digested overnight at 37ºC with 1 mg dm^{-3} Endo III or Fpg in TE buffer (10 mM Tris-HCl, and 1 mM EDTA) containing 100 mM NaCl and 0.1 g dm^{-3} bovine serum albumin. The plugs were then washed twice in TE buffer, and each plug was inserted into a separate well of a 0.6% (w/v) agarose gel. The gel was electrophoresed for 20 h in TBE buffer consisting of 89 mM Tris, 89 mM boric acid, and 2 mM EDTA under a constant current of 17 mA. The images of gels stained with EtBr were captured by a camera system equipped with a UV

trans-illuminator. The captured images were analyzed by ImageJ software (National Institute of Health, United States) [Rasband, 2012]. The fraction of chromosomal DNA damage was calculated by measuring the fluorescence intensities of DNA observed in the gel images; the proportion of DNA fragments migrating out of each plug to those remaining in the plug. The damaged DNA in this analysis indicates the DSB fraction formed in the total chromosomal DNA.

2.5.2. Mass spectrometric analysis of oxidative base lesions

Chromosomal DNA was extracted from 10 cm^3 plasma-treated *E. coli* cells with a DNeasy Blood & Tissue Kit (Qiagen, Netherlands), after the exposure to plasma at the treatment times of 0, 12, 48, and 96 s as described in *Section 2.2*. The extracted chromosomal DNA was hydrolyzed in 0.1 cm^3 solution with 3 U of nuclease P1 at 37°C for 60 min to obtain the nucleotide components. The mixture was next hydrolyzed with 1.2 U of alkaline phosphatase in Tris-HCl (pH 8.5) at 37°C for 60 min for nucleoside preparation. L-8-OH-dG or L-5-OH-dC reagent was added to the mixture as an internal standard, and the samples were then passed through a Nanosep Filter Centrifugal Device (Pall, United States).

MS analysis of oxidative base lesions was performed by LC-MS/MS, using an LCMS-8030 instrument (Shimadzu, Japan), as described in Chapter 1. The nucleoside mixtures were separated at 40°C on a KINETEX 1.7-μm C18 column (ϕ 2.1 mm × 100 mm: Phenomenex, United States) with an isocratic mobile phase of 0.1% (v/v) aqueous formic

acid containing 5% (v/v) acetonitrile. MS data acquisition was performed in MRM mode. For 8-OH-dG with L-8-OH-dG, the collision energies were optimized at 15 eV and 16 eV, and the MRM transitions were from 284 to 168 m/z and from 289 to 173 m/z, corresponding to the precursor ion and the product ion, respectively. For 5-OH-dC with L-5-OH-dC, the collision energies were optimized at 12 eV and 13 eV, and the MRM transitions were from 244 to 128 m/z and from 247 to 131 m/z, corresponding to the precursor ion and the product ion, respectively. Chromosomal DNA from *E. coli* cells irradiated with γ-rays was analyzed as just described.

2.6. DNA sequencing analysis

pUC19 DNA was treated by the pulsed discharge at ~100 mJ cm^{-3}, which corresponds to the treatment time of 6 s, leaving ~10% supercoiled DNA, as estimated by agarose-gel analysis described in Chapter 1. Ten nanograms of the treated DNA were transfected into *E. coli* JM109 competent cells (10^9 cfu cm^{-3}) by heat-shock. The cell suspension was diluted in PBS and spread onto an LB agar plate containing 50 mg dm^{-3} ampicillin, 0.4% (w/v) 5-bromo-4-chloro-3-indolyl β-D-galactopyranoside (X-gal), and 2% (w/v) isopropyl β-D-thiogalactopyranoside. pUC19 plasmid encodes a *lacZα* gene, and the *E. coli* JM109 host strain expresses *lacZ*ΔM15. Co-expression of both *lacZα* and *lacZ*ΔM15 leads to full activity of the *lacZ* gene product (α-complimentation) [Hoebee et al., 1988], and X-gal is degraded to a blue-colored product, which leads to the formation of blue colonies. Therefore, inactivating base alterations in the

pUC19 *lacZα* gene leads to the formation of white colonies. I cloned white colonies. Plasmid DNAs from white colonies were extracted with a QIAprep Spin Miniprep Kit (Qiagen, Netherlands), and *lacZα* sequences were analyzed with an ABI PRISM 310 Genetic Analyzer, using BigDye Terminator Cycle Sequencing Kit (Applied Biosystems, United States). The sequencing primers used were 5′-GCTTGTCTGTAAGCGGATGC-3′ and 5′-GCGGGCAGTGAGCGCAACGC-3′. DNA irradiated with γ-rays for 5 mJ cm^{-3} were analyzed in the same way, which included an equivalent 10% supercoiled fraction following the pulsed discharge, as mentioned above.

3. Results

3.1. Measurement of ROS induced by pulsed discharge

The yields of OH radical and H_2O_2 were estimated after the plasma treatment. The OH radical concentrations in pulsed discharge-treated water were 5.1 ± 2.4, 10.4 ± 2.0, 18.7 ± 2.1, and 29.6 ± 1.7 nmol cm^{-3}, corresponding to mean values ± SD, at applied energies of 157, 313, 626, and 1253 mJ cm^{-3}, respectively (Fig. 2-3a). The OH radical concentrations in aqueous solution irradiated with γ-rays were 2.7 ± 0.1, 5.4 ± 0.1, 13.4 ± 0.5, and 26.8 ± 0.7 nmol cm^{-3} at applied energies of 10, 20, 50, and 100 mJ cm^{-3}, respectively (Fig. 2-3b). There was no detected OH radical without any treatments.

H_2O_2 concentrations in water samples treated with the pulsed discharge were 17.6 ± 0.1, 36.3 ± 0.1, 65.7 ± 0.4, and 121.9 ± 0.7 nmol cm^{-3} at applied energies of 188, 377, 754, and 1507 mJ cm^{-3}, respectively (Fig. 2-4a). In contrast, the H_2O_2 concentrations following γ-irradiation were 2.0 ± 0.2, 4.1 ± 0.1, 9.5 ± 0.2, and 17.9 ± 0.3 nmol cm^{-3} at applied energies of 10, 20, 50, and 100 mJ cm^{-3}, respectively (Fig. 2-4b). The background concentration of H_2O_2 was between 0.5–0.9 nmol cm^{-3} without any treatments.

3.2. Viability of E. coli cells treated by pulsed discharge

E. coli KA796 cell viabilities were 70.4 ± 4.5, 45.9 ± 4.8, 27.4 ± 3.1, and 9.7 ± 1.8% following the pulsed discharge treatment at applied energies

of 180, 361, 721, and 1443 mJ cm^{-3}, respectively (Fig. 2-5a). The cell viabilities for γ-irradiated cells were 103.7 ± 1.7, 97.8 ± 1.5, 48.6 ± 3.5, and 4.3 ± 0.2% at applied energies of 10, 20, 50, and 100 mJ cm^{-3}, respectively (Fig. 2-5b).

3.3. Chromosomal DNA damage in E. coli cells treated by pulsed discharge

Chromosomal DNA damage in *E. coli* cells exposed to the plasma were analyzed by SFGE (Fig. 2-6a). Two dm^3 of *E. coli* cell suspension was exposed to the plasma at room temperature, and aliquots of treated cell suspension were sampled every 24 seconds for up to 96 seconds. The SFGE results indicated that DSB fraction increased with increasing the applied energy of the pulsed discharge. Enzymatic treatments with Endo III and Fpg detected oxidative base lesions in damaged DNA, as these glycosylases recognized oxidative pyrimidines and purines, such as TG and 8-OH-G, respectively, and incised the DNA strands at the damaged sites [Terato et al., 2008]. Damaged DNA corresponding to DSB caused by the pulsed discharge were 1.8 ± 2.5, 7.0 ± 4.1, 9.6 ± 4.7, and 16.9 ± 4.9% of total chromosomal DNA at applied energies of 310, 620, 940, and 1250 mJ cm^{-3}, respectively (Fig. 2-6a). Damaged DNA corresponding to Endo III-sensitive site caused by the pulsed discharge were 3.5 ± 4.5, 10.6 ± 3.6, 24.4 ± 8.2, and 28.8 ± 5.5% of the total DNA at the corresponding applied energies. The damaged DNA corresponding to Fpg-sensitive site caused by the pulsed discharge were 4.5 ± 3.5, 18.8 ± 5.3, 21.9 ± 4.2, and 28.6 ± 4.6%

of the total DNA at the corresponding applied energies. In contrast, the amount of damaged DNA with DSBs caused by γ-rays were 1.4 ± 0.6, 4.6 ± 2.7, 6.3 ± 2.5, and 8.5 ± 1.1% of the total DNA at applied energies of 25, 50, 75, and 100 mJ cm^{-3}, respectively (Fig. 2-6b). The prevalence of damaged DNA detected as Endo III-sensitive sites caused by γ-rays were 2.1 ± 2.0, 5.0 ± 1.6, 8.6 ± 3.3, and 11.5 ± 3.0% of the total DNA, respectively, at the corresponding applied energies. The percent of damaged DNA with Fpg-sensitive sites caused by γ-rays were 4.4 ± 1.6, 8.2 ± 3.9, 14.5 ± 4.5, and 18.0 ± 4.3%, respectively, at the corresponding applied energies.

3.4. Measurements of oxidative base lesions induced by pulsed discharge

The SFGE results indicated that the pulsed discharge induced oxidative base lesions in treated bacterial cells. I measured quantitatively 8-OH-G (8-OH-dG) and 5-OH-C (5-OH-dC) in the chromosomal DNA extracted from plasma-treated *E. coli* cells by LC-MS/MS, because 8-OH-G and 5-OH-C are major oxidative base lesions induced by ionizing radiation and Fenton reaction [Rivière et al., 2006; Wagner et al., 1992]. The calibration curves with both lesion standards were linear within the range of 0.1–10 ng cm^{-3} (seven-point calibration, $|r^2| > 0.999$). During LC separation, the peaks of 5-OH-dC and 8-OH-dG appeared 1.6 and 2.2 min later after injection, respectively (Fig. 2-7a). The peak heights for both lesions increased in direct proportion to increases in the applied energy of the pulsed discharge. In plasma-exposed *E. coli* chromosomal DNA,

8-OH-dG yields were 3.9 ± 0.3, 5.8 ± 1.0, 7.6 ± 0.4, and 15.6 ± 2.3 nucleosides in 10^5 dG, and 5-OH-dC yields were 6.9 ± 1.9, 14.1 ± 6.8, 41.6 ± 1.1, and 106.2 ± 24.8 nucleosides in 10^5 dC (equal to 10^5 dG), at applied energies of 0, 186, 744, and 1488 mJ cm^{-3}, respectively (Fig. 2-7b). In γ-irradiated *E. coli* cells, 8-OH-dG yields with chromosomal DNA were 2.4 ± 0.3, 3.2 ± 0.7, 7.5 ± 1.0, and 10.8 ± 2.3 nucleosides in 10^5 dG, and 5-OH-dC yields were 3.5 ± 0.5, 3.9 ± 1.6, 14.4 ± 0.3, and 18.8 ± 4.2 nucleosides in 10^5 dC, at applied energies of 0, 10, 50, and 100 mJ cm^{-3}, respectively (Fig. 2-7c). These yields were calculated as 50.8% GC content of the *E. coli* cells chromosomal DNA from the procedure as described previously [Pouget et al., 2002]. The initial production rates of 8-OH-dG and 5-OH-dC in plasma-treated *E. coli* measured with chromosomal DNA were 1.2 nucleosides in 10^7 dG per mJ cm^{-3} and 3.9 nucleosides in 10^7 dC per mJ cm^{-3}, respectively. The corresponding rates in γ-irradiated *E. coli* chromosomal DNA were 8.5 nucleosides in 10^7 dG per mJ cm^{-3} and 4.0 nucleosides in 10^7 dC per mJ cm^{-3}, respectively.

3.5. DNA sequencing analysis for oxidative base lesions

Base change frequencies in *lacZα* gene of treated pUC19 plasmid DNA were estimated to be 2.2×10^{-4}, with an associated survival of 74.5% in the pulsed discharge experiments. The base change frequencies and survival rate following exposure to γ-rays were 5.0×10^{-4} and 64.0%, respectively. Both the pulsed discharge and γ-rays induced mainly base substitutions (Table 2-1). The most predominant change was G:C to A:T

transition (64.5%), and the second was A:T to G:C transition (29.0%) in the plasma-induced *lacZα* alteration. G:C to T:A transversions (3.2%) and 1-base deletions (3.2%) occurred more rarely than the above events. The major base-change sites were C305, C306, G325, C365, and T369 following the pulsed discharge exposure (Fig. 2-8a). In γ-irradiated bacterial cells, a half of base changes occurred at G:C base pairs, which consisted of G:C to A:T transitions (24%), G:C to T:A transversions (8%), and G:C to C:G transversions (8%). ~30% of the base changes were at A:T base pairs, which consisted of A:T to G:C transitions (16%) and A:T to T:A transversions (16%) for γ-rays. Also, 1-base deletions, most of which were located at position 422 in the *lacZα* gene, accounted for 28% of the DNA alterations identified in γ-irradiated cells (Fig. 2-8b).

4. Discussion

Pulsed discharge with cavitation causes DNA damage, which is thought to be a key factor underlying its sterilizing effects. My result using DNA molecule targets in Chapter 1 supports this potential mechanism. Then, I quantitated the ROS production and DNA damage following the pulsed discharge treatment, and discussed the involvement of ROS in the bactericidal ability of the pulsed discharge, especially OH radical and H_2O_2 were measured, because both are typical ROS formed by exposure to the plasma [Jiang et al., 2014]. These ROS exert bactericidal effects by damaging cellular targets including DNA [Takemoto et al., 1998]. The OH radical and H_2O_2 concentrations induced by the plasma were directly proportional to the applied energy. OH radical production from the plasma exposure reached ~30 nmol cm^{-3} at an applied energy of 1250 mJ cm^{-3} (Fig. 2-3a), which was comparable to that produced by γ-irradiation at an applied energy of 100 mJ cm^{-3} (Fig. 2-3b). Therefore, the efficiency of OH radical generation following the pulsed discharge is approximately one-tenth that of γ-ray exposure. The electrical conductivity affects OH radical generating efficiency in the plasma [Sahni and Locke, 2006; Sun et al., 1997]. Before discharge treatment, I measured the electrical conductivities of experiment solutions with WM-22EP (TOA DDK, Japan), typically resulting in 8.5 mS m^{-1} and 60 mS m^{-1} in aqueous NaTA experiment solution and *E. coli* suspension, respectively. While OH radical concentrations in both solutions showed no difference in the range of discharge power in my experiment. There were ~30 μM of OH radical in both solutions after the

plasma-treatment of 96 seconds. Thus, the differences of conductivity and discharge power seem to have no influence the results in my experiment. On the other hand, H_2O_2 production following the plasma treatment reached ~120 nmol cm^{-3} at an applied energy of ~1500 mJ cm^{-3}, which was 6-7 fold greater than that obtained by γ-irradiation at 100 mJ cm^{-3} (Figs. 2-4a and 2-4b). The efficiency of H_2O_2 generation after the pulsed discharge exposure was similar as γ-rays induced one at the same applied energy. H_2O_2 is formed by two OH radicals reacting with each other [Jiang et al., 2014]. Thus, OH radical will convert to H_2O_2 more easily in the plasma than in γ-irradiated water. My data indicate that the plasma was in fact generated in my apparatus, given that characteristic emission spectra (Fig. 2-2) and electrical breakdown (Fig. 2-1b) were observed. Using this apparatus, I adopted a bubbling system for energy-efficient plasma generation [Miichi et al., 2002; Shih and Locke, 2009]. This resulted in a limited localization of ROS induced by the plasma at the interface between bubble and water in treated fluids. When OH radicals are formed only in the plasma channel of 1 mm diameter in between electrodes, the local concentration of OH radical is calculated to be more than 20 mM in this region. Thus, such concentrated OH radical will react each other with high efficiency, and then H_2O_2 are generated. This finding is consistent with the results of a previous study [Gupta and Bluhm, 2007]. ROS localization is a key factor associated with cellular DNA damage.

The viability of *E. coli* cells following the pulsed discharge treatment decreased exponentially with the applied energy, reaching <10%

at 1400 mJ cm^{-3} (Fig. 2-5a). This viability was nearly equivalent to that observed with γ-rays at an applied energy of 100 mJ cm^{-3} (Fig. 2-5b). I investigated whether this decrease in viability was responsible for oxidative DNA damage. Electrophoretic analysis revealed the generation of oxidative DNA damage, such as DSB and oxidative base lesions, in the chromosomal DNA of plasma-treated *E. coli* cells (Fig. 2-6a). I used Endo III and Fpg to detect oxidative base lesions. Endo III recognizes and excises oxidative pyrimidine lesions in DNA, such as TG, 5-OH-C, 5-hydroxy-uracil (5-OH-U), and 5-formyluracil (5-foU) [Ali et al., 2004; Hatahet et al., 1993; Hatahet et al., 1994]. The increase in Endo III-sensitive sites indicated that such damage were introduced into the chromosomal DNA of treated *E. coli* cells. Fpg recognizes and excises oxidative purine lesions in DNA, including 8-OH-G and imidazole ring-opened products such as Fapy-G and Fapy-A [Boiteux et al., 1992; Haraguchi and Greenberg, 2001; Tchou et al., 1991; Tchou et al., 1994]. A previous study reported that Fapy-G yield was similar to 8-OH-G yield following oxidative stresses, such as γ-irradiation, although Fapy-A yield was significantly smaller than those of 8-OH-G and Fapy-G [Boiteux et al., 1992; Pouget et al., 2002]. Thus, the increase in Fpg-recognition sites indicates the presence of 8-OH-G and Fapy-G. I compared damage yields obtained with the pulsed discharge at 1250 mJ cm^{-3} and γ-rays at 100 mJ cm^{-3}, both of which reduced the viability of *E. coli* cells to 10% (Fig. 2-5). DSB yield following the pulsed discharge treatment was superior to that from γ-ray exposure at the same applied energies. The yield of oxidative purine lesions with the

pulsed discharge method was 12.6%, which was calculated by subtracting the DSB yield from that relating to Fpg-sensitive sites. γ-irradiation resulted in 9.5% damaged DNA with oxidative purine lesions. The yields of oxidative pyrimidine lesions were calculated as 13.0% after the pulsed discharge treatment and 3.3% after γ-irradiation. Thus, the pulsed discharge can induce oxidative pyrimidine lesions more efficiently than γ-rays, as discussed in greater detail below.

I then mass-spectrometrically analyzed the formation of 8-OH-G and 5-OH-C as signature base lesions induced by oxidation factors such as ionizing radiation. MS analysis of digested chromosomal DNA in the plasma-treated cells indicates that the amounts of 8-OH-G and 5-OH-C increased in proportion to the applied energy of pulsed discharge (Figs. 2-7b and 2-7c). 8-OH-G and 5-OH-C were formed through OH radical attacking to C-8 position of guanine and 5,6-double bond of cytosine, respectively [Kasai and Nishimura, 1984; Wagner and Cadet, 2010]. Thus, OH radical oxidizes cellular DNA, as these oxidative base lesions were generated. The initial production rate of 5-OH-C by the plasma was about 4-fold greater than that of 8-OH-G. H_2O_2 treatment with ascorbate leads to 5-OH-C and 8-OH-G generation, and the 5-OH-C yield was significantly higher than the 8-OH-G yield in Jurkat cell [Rivière et al., 2006]. Compared to the respective lesion yields after a pulsed discharge exposure of 1500 mJ cm^{-3} and γ-rays exposure of 100 mJ cm^{-3}, based on the applied energy required to reduce the viability to ~10%, 5-OH-C yield of the pulsed discharge was ~5-fold greater than that of γ-rays. On the other hand,

8-OH-G yield for pulsed discharge was almost equal with that for ^{137}Cs γ-rays. The DNA sequence analysis result is similar to the MS analysis result for 5-OH-C and 8-OH-G generation in DNA plasmid treated by the pulsed discharge. I found a 3.2% G:C to T:A transversion rate, which was observed for all base changes induced by the plasma (Table 2-1). G:C to T:A transversion is responsible for 8-OH-G mispairing during DNA synthesis. These findings indicate that 8-OH-G was formed in plasma-treated DNA. The most predominant base change was G:C to A:T transition (64.5%). 5-OH-C promotes mutagenesis by triggering G:C to A:T transitions, and the mispairing with 5-OH-C was significantly higher than with other base lesions, such as TG and 8-OH-G [Feig et al., 1994]. Additionally, 5-OH-C is prone to deamination resulting in 5-OH-U, which has similar mutagenic potential [Wagner et al., 1992]. Since 5-OH-U is more stable than 5-OH-C, 5-OH-C shows its mutagenic ability directly and indirectly via 5-OH-U. Thus, G:C to A:T transitions attribute to oxidative cytosine formation induced by the plasma. The second predominant base change was A:T to G:C transition (29%). That is thought to be result from oxidized thymine moieties, such as 5-foU [Zhang, 2001]. Unfortunately, I have no appropriate standard substances for 5-OH-U and 5-foU, and further investigation is needed regarding pyrimidine oxidation by the plasma. The overall proportion of transitions obtained by γ-irradiation was 40%, which was significantly smaller than that induced by the pulsed discharge (Table 2-1).

The yield ratio of 5-OH-C to 8-OH-G following the pulsed

discharge was calculated as 6.8 at an applied energy of 1500 mJ cm^{-3} from MS results (Fig. 2-7b). However, the yield ratio of 5-OH-C to 8-OH-G after γ-irradiation was 1.7 at an applied energy of 100 mJ cm^{-3}, which was associated with an *E. coli* viability similar to pulsed discharge treated cells (Figs 2-5 and 2-7c). Electrophoretic and DNA sequence analyses conducts us similar conclusion. The pulsed discharge preferred to induce 5-OH-C but not 8-OH-G unlike ionizing radiations. γ-irradiation is usually found to cause G:C to T:A transversion as a major base change [Braun et al., 1997; Kuipers et al., 1999], indicating that 8-OH-G is a major base lesion formed by γ-irradiation. Fapy-G is another major oxidative guanine lesion, and can inhibit DNA polymerase progression, but is weakly mutagenic in *E. coli* cell [Patro et al., 2007]. Because my present electrophoretic analysis did not discriminate 8-OH-G and Fapy-G for guanine oxidation, I could not determine how much ROS were consumed for Fapy-G generation overwhelming 8-OH-G generation after the pulsed discharge and γ-irradiation, respectively. When OH radical attacks the C-8 position of guanine, 8-hydroxy-7,8-dihydroguanyl radical is formed, which thereafter is converted to Fapy-G and 8-OH-G via reduction and oxidation reactions, respectively [Cadet et al., 2010]. Oxidative purine lesions induced by γ-irradiation probably contain 8-OH-G more abundantly than Fapy-G. On the other hand, the pulsed discharge could induce Fapy-G more abundantly than 8-OH-G. O_2 is involved in the oxidation of 8-hydroxy-7,8-dihydroguanyl radical under oxic conditions (the oxygen effect) [Cadet et al., 2010]. Cavitation during the pulsed discharge well

mixes ROS and dissolved O_2 molecules in treated solutions. Thus, O_2 consumption during the pulsed discharge will be larger than that during γ-irradiation. Therefore, I consider that the pulsed discharge induces smaller oxidation of 8-hydroxy-7,8-dihydroguanyl radical, resulting in increase of Fapy-G formation. I need a further analysis for Fapy-G yield from the pulsed discharge.

When energetic electrons react with H_2O and O_2 in the plasma boundary, various active species are produced, such as OH radical, H_2O_2, O, $^1O_2$, $\cdot O_2^-$, and water radical ion (H_2O^+) [Gupta and Bluhm, 2007; Jiang et al., 2014]. Reactive species such as OH radical, $^1O_2$, and O have very short half-lives. Therefore, such species can reach the chromosomal DNA only when they are generated close to DNA. However, most reactive species appear to be localized in solution on the outside of cells during the pulsed discharge treatment, as they are locally generated in the plasma. Further, most highly reactive polar or charged species generated outside of cells, such as OH radical, $^1O_2$, O, $\cdot O_2^-$, and H_2O^+ cannot pass through cell membrane and cannot reach the cellular DNA. In contrast, H_2O_2 is electrically neutral and very stable in water. The maximal concentration of H_2O_2 in this study was ~120 nmol cm^{-3}. When pUC19 plasmid DNA were treated with H_2O_2 ranging from 4 to 4000 mM for 10 minutes, I found no DNA damage detected in the agarose gel electrophoresis at all (data not shown). Thus, the concentration of H_2O_2 in this experiment seems to be insufficient to cause lethal damage to cellular DNA, and by extension, bactericidal effect on *E. coli* cells [Takemoto et al., 1998]. However, H_2O_2

can enter cells due to its electric neutrality, and then is capable of converting to more active species, such as OH radical via interaction with UV radiation or abundant cellular metal ions [Sato, 2009; Walling, 1975]. Synergistic bactericidal effects of H_2O_2 and UV have been reported [Hartman and Eisenstark, 1978]. The involvement of H_2O_2 in cellular DNA damage can explain the high yield of DNA-damaging species induced by the pulsed discharge. H_2O_2 treatment with ascorbate promotes a significantly higher yield of 5-OH-C yield than 8-OH-G [Rivière et al., 2006]. In addition, one study reported that H_2O_2 treatment led to the formation of more oxidative pyrimidine lesions than oxidative purine lesions in cellular DNA, using a comet assay [Kruszewski and Iwanenko, 2003]. These studies suggest that H_2O_2 augments oxidative DNA damage caused by the pulsed discharge and that ROS invading from outside the cell membrane induce oxidative pyrimidine lesions more efficiently than purine lesions. $^1O_2$ can also traverse the cell membrane and oxidize chromosomal DNA to cause oxidative DNA damage, such as DSB and oxidative base lesions [Gorman et al., 1976; Toyooka et al., 2006]. In this study, I did not investigate $^1O_2$ generation, and its involvement in DNA damaging. During the pulsed discharge treatment, the most of active species are generated outside the cell, which will be consumed through reactions with surrounding molecules and atoms. In contrast, γ-rays can directly generate ROS within the interior of cells, resulting in directly oxidizing of cellular DNA with higher efficiency. Thus, while most ROS induced by the pulsed discharge must pass through cell membranes to attack the chromosomal

DNA, those induced by γ-irradiation can directly attack chromosomal DNA without passing through membrane. Since only a fraction of extracellularly generated ROS can proceed into cell pass through cell membrane, the bactericidal effect of the pulsed discharge is significantly lesser energy-efficient than γ-rays. Hydrodynamic cavitation itself can show sterilizing effect by generating a local high pressure and temperature [Jyoti and Pandit, 2001]. However, these effects were marginal in my apparatus with the shorter treatment times (Chapter 1). In my system, the electric field probably kept in very short period before each pulsed electric discharge starting, and its strength was insufficient for the sterilizing effect [Sale and Hamilton, 1967] (Chapter 1). Thus, the electric field seems not to be involved in DNA damage in the treated *E.coli* cells in this study. Temperature also kept out of the damaging. Water temperature was raised from 25 to 28°C after 96 s treatment in my system, which was thought to not influence the bacterial viability and the formation of oxidative DNA damages.

Figures and Table

Table 2-1 Classification of base changes in the *lacZα* gene following the pulsed discharge and ^{137}Cs γ-rays.

Mutations		Number of occurrences			
		Pulsed discharge		^{137}Cs γ-rays	
Base-pair substitutions			(%)		(%)
Transitions:	A:T→G:C	9	(29.0)	4	(16.0)
	G:C→A:T	20	(64.5)	6	(24.0)
Transversions:	G:C→T:A	1	(3.2)	2	(8.0)
	G:C→C:G	-	-	2	(8.0)
	A:T→C:G	-	-	-	-
	A:T→T:A	-	-	4	(16.0)
Deletions:	Single deletion	1	(3.2)	7	(28.0)
Total		31	(100.0)	25	(100.0)

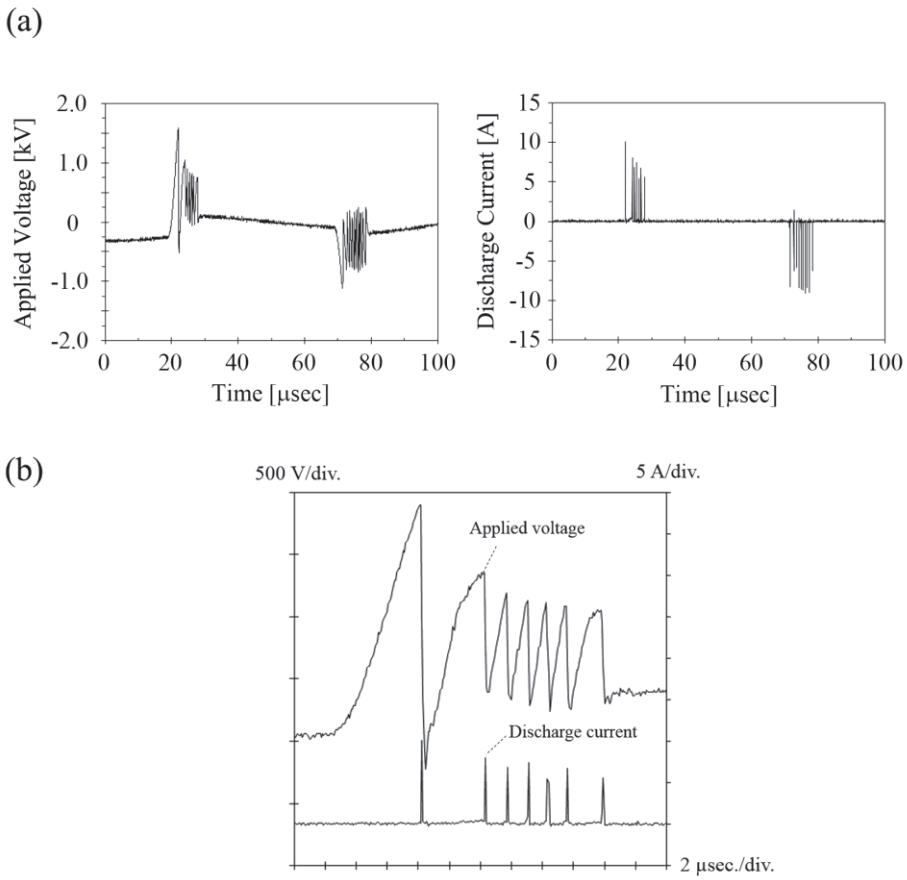

Figure 2-1. (a) Typical waveforms of applied voltages (left panel) and discharge currents (right panel) are shown during discharge of the power supply at a frequency of 10 kHz. (b) Enlarged view of both waveforms ranging from 18 to 30 μsec in Fig. 2-1a. The electrical breakdown indicating the plasma generation is caused by the application of voltage, and then a pulse-like discharge current generates intermittently.

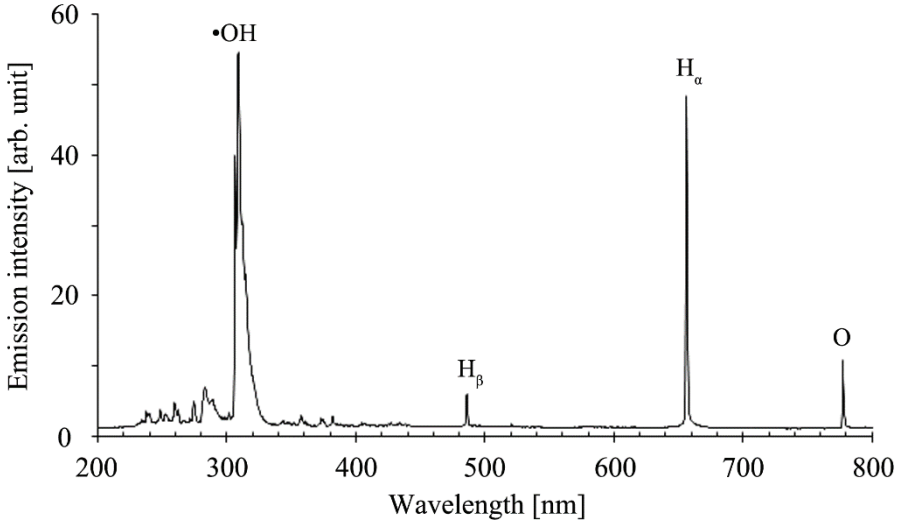

Figure 2-2. Light emission spectrum from the plasma generated by the pulsed discharge. In the spectrogram, ·OH, $H_{\alpha,\beta}$, and O designate the emission peaks from OH radical, atomic hydrogen and atomic oxygen, respectively. Arbitrary units were used to calculate signal ratios relative to the background. Some minor peaks in UVC region are derived from excitation of metals, such as iron, constituting stainless steel needle electrodes, and the peak of 282 nm-wavelength is derived from the $A^2\Sigma^+$-to-$X^2\Pi$ (v = 1, 0) transition of OH radical [Sun et al., 1997].

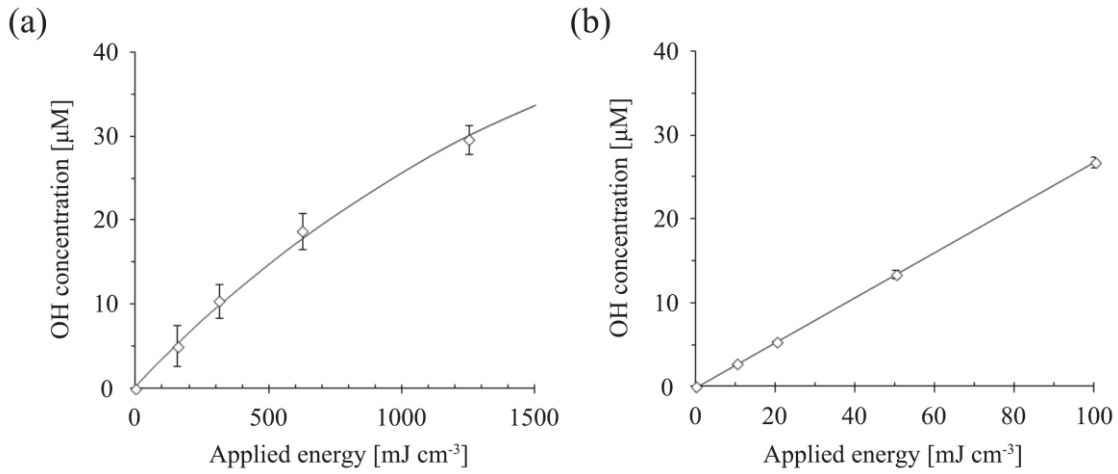

Figure 2-3. OH radical concentrations generated by the pulsed discharge (a) and ^{137}Cs γ-rays (b). The data shown are expressed as mean ± SD of 3 experiments performed in triplicate. In some cases, the error bars are small enough to be masked behind the associated graph symbols. The applied energies of the pulsed discharge were calculated from the associated discharge powers and exposure times. This experiment was performed with ~30W of discharge power. The applied γ-rays energies were calculated from the absorbed dose, assuming that water density is $\rho = 1.0$ g cm^{-3}, and thus, the applied energy of ^{137}Cs γ-rays is nearly equivalent to the dose (Gy).

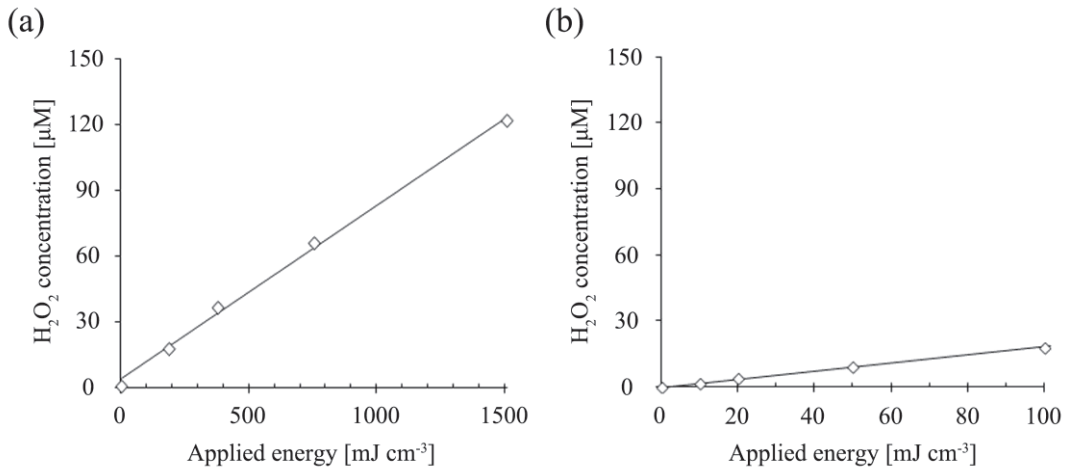

Figure 2-4. H_2O_2 concentrations generated by the pulsed discharge (a) and ^{137}Cs γ-rays (b). The data shown are expressed as mean ± SD from triplicate experiments. In some cases, the error bars are small enough to be masked behind the associated graph symbols. The applied energies of the pulsed discharge were calculated from the associated discharge powers and exposure times. This experiment was performed with ~30W of discharge power. The applied γ-rays energies were calculated from the absorbed dose, assuming that water density is $\rho = 1.0$ g cm^{-3}, and thus, the applied energy of ^{137}Cs γ-rays is nearly equivalent to the dose (Gy).

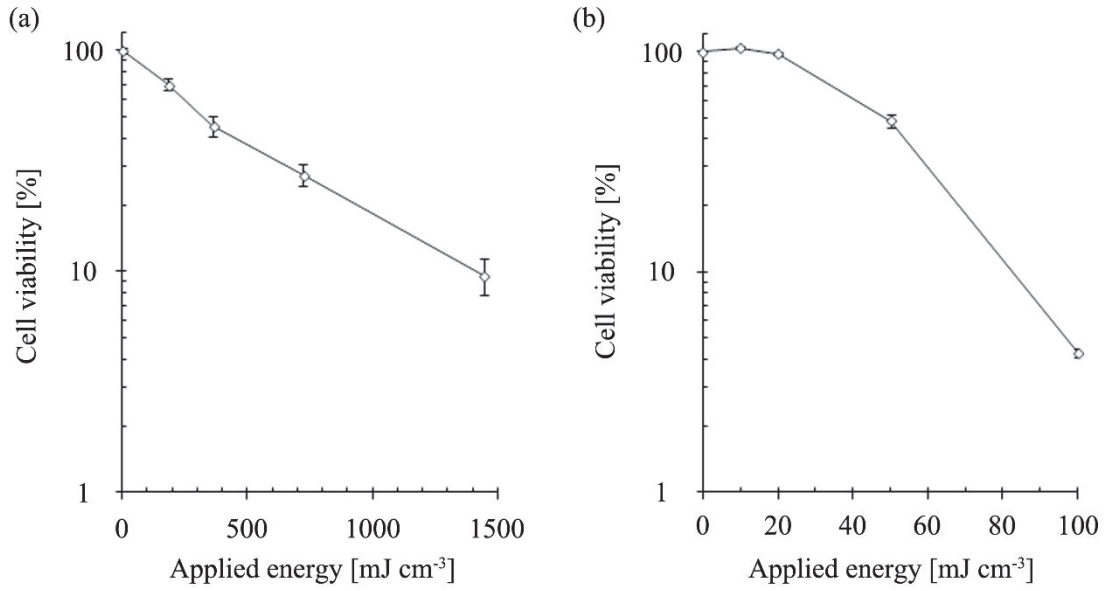

Figure 2-5. Cell viability of *E. coli* KA796 cells following exposure to the pulsed discharge (a) or ^{137}Cs γ-rays (b). The respective data are expressed as mean ± SD from triplicate experiments. In some cases, the error bars are small enough to be masked behind the associated graph symbols. The pulsed discharge experiments were performed with ~30W of discharge power. The applied γ-rays energies were calculated from the absorbed dose, assuming that water density is $\rho = 1.0$ g cm^{-3}. Then, the applied energy of ^{137}Cs γ-rays was equivalent to the absorbed dose (Gy).

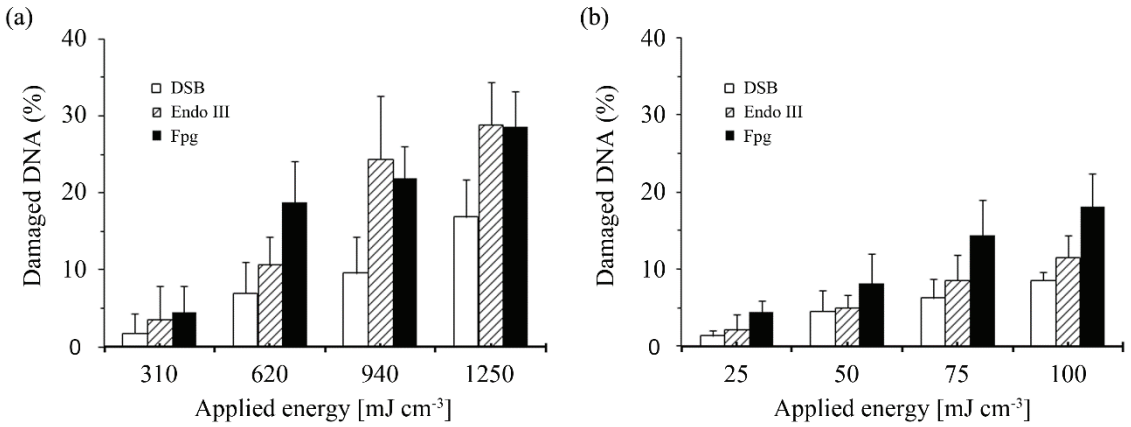

Figure 2-6. Chromosomal DNA damage to *E. coli* cells treated by the pulsed discharge (a) and ^{137}Cs γ-rays (b). The open, striped and closed bars represent DSBs (no enzyme treatment), Endo III-sensitive sites, and Fpg-sensitive sites, respectively. The respective data are expressed as mean ± SD from 3 independent experiments. The pulsed discharge experiments were performed with ~26W of discharge power. The applied energy of ^{137}Cs γ-rays was equivalent to the absorbed dose (Gy).

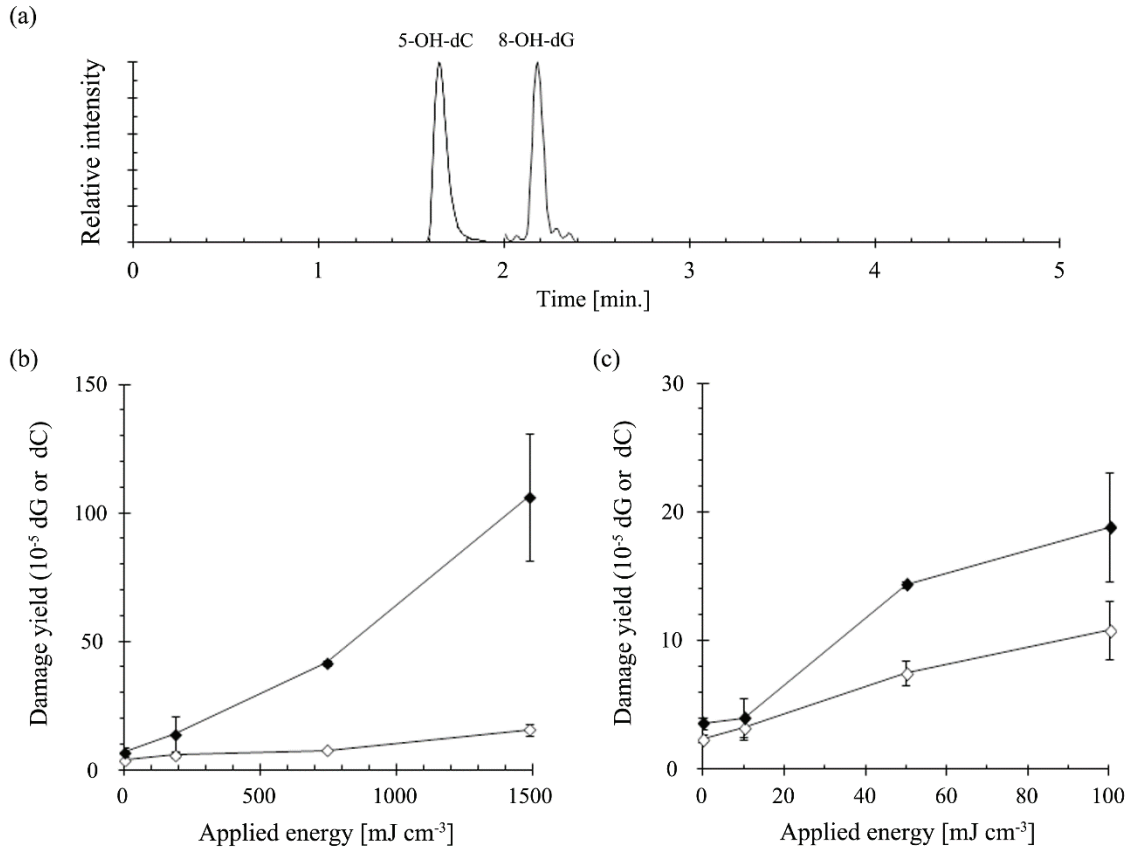

Figure 2-7. MS data of oxidative base lesions. LC-MS/MS profiles of 5-OH-dC and 8-OH-dG alterations detected in extracted *E. coli* chromosomal DNA treated by the pulsed discharge (a). The retention times of 5-OH-dC and 8-OH-dG were 1.6 and 2.2 min, respectively. The yields of 5-OH-dC and 8-OH-dG in extracted chromosomal DNA from *E. coli* cells treated by the pulsed discharge (b) and ^{137}Cs γ-rays (c). The open and closed circles represent the yields of 8-OH-dG and 5-OH-dC, respectively. The respective data are expressed as mean ± SD from triplicate experiments. The pulsed discharge experiments were performed with ~30W of discharge power. The applied energy of ^{137}Cs γ-rays was equivalent to the absorbed dose (Gy).

Figure 2-8. DNA sequences of the *lacZα* gene (324 bp) in plasmid progeny DNA exposed to the pulsed discharge (a) and ^{137}Cs γ-rays (b). The respective characters below the sequences represent base changes and single deletions (Δ).

General Conclusion

In this thesis, I study the bactericidal mechanism of pulsed discharge with cavitation. Some other studies indicate that the bactericidal effect by the plasma is related to ROS [Bai et al., 2010; Kadowaki et al., 2009; Sato et al., 1996], and suggest that DNA is an important target of the effect [Chen et al., 2008; Kadowaki et al., 2009]. Therefore, I here estimate the yields of ROS and oxidative DNA damage after treatment of the pulsed discharge.

In Chapter 1, I show the result of analysis of pUC19 plasmid DNA exposed by the pulsed discharge. It is shown that the yields of DNA strand breaks including both SSB and DSB, and 8-OH-G harboring in treated DNA substrates increased with the applied energy. I also discuss the relationship between the cell viability and chromosomal DNA damage by using *E. coli* strains lacking *mutM* gene that is responsible for the repair of 8-OH-G. As a result, it is found that lack of *mutM* sensitizes the host bacterial cells, and the yield of DSB increases with the applied energy in the chromosomal DNA of the treated *E. coli* cells. These data indicate that oxidative DNA damage caused by the pulsed discharge is inextricably related with the bactericidal effect.

In Chapter 2, I confirm the ROS generation by the pulsed discharge, and obtain the further evidence about oxidative DNA damaging in the treated cells. In result, the pulsed discharge generates various active species containing OH radical and H_2O_2 in the treated aqueous solution. Also, the pulsed discharge induces oxidized base lesions containing 8-OH-G and 5-OH-C as well as DNA strand breaks in the treated *E. coli* cells. These

results indicate that the pulsed discharge generates extra-cellular ROS, such as OH radical and H_2O_2, some of which penetrate into cell membrane, leading to oxidative DNA damages in *E.coli* cells. Therefore, I consider that the pulsed discharge causes DNA damage, the most critical in terms of cell survival, and it results in the bactericidal effect via the plasma-induced ROS.

My present result indicates that ROS are generated by the pulsed discharge, and that oxidative DNA damages are yielded at the same time as ROS generating. Thus, I conclude that the pulsed discharge expresses its bactericidal effect via oxidative stress through the plasma generation. Before my study, various factors are thought to take part in the effect, such as electric field, shockwaves and UV, as well as ROS. Therefore, my study will make a substantial contribution in plasma application.

My study shows valuable information for the practical use of plasma in this matter, but it leaves unexplained mechanism of attacking to DNA of ROS generated by the plasma out of cell. Extracellular generated OH radical cannot react with the DNA inside cell because of its very short lifetime. On the other hand, H_2O_2 can intrude into cell. I investigate the relative higher yield of H_2O_2 from the discharged plasma than ionizing radiation. One possible mechanism of damaging DNA is intracellular conversion of H_2O_2 to more active species such as OH radical after the penetration, that is accelerated by intracellular existing metals, termed as Fenton like reaction. UV generated from the plasma also assists that conversion.

Although there has been an unsolved point, I elucidate the most mechanism of bactericidal effect from the pulsed discharge, and this meaningful outcome can be used for it efficient application.

References

Ali M.M., Kurisu S., Yoshioka Y., Terato H., Ohyama Y., Kubo K., Ide H., Detection of endonuclease III- and 8-oxoguanine glycosylase-sensitive base modifications in γ-irradiated DNA and cells by the aldehyde reactive probe (ARP) assay, *J. Radiat. Res.* **45** (2004) 229-237.

Appleby A., Schwarz H.A., Radical and molecular yields in water irradiated by γ rays and heavy ions, *J. Phys. Chem.* **73** (1969) 1937-1941.

Armstrong W.A., Facey R.A., Grant D.W., Humphreys W.G., A tissue-equivalent chemical dosimeter sensitive to 1 rad, *Can. J. Chem.* **41** (1963) 1575-1577.

Asagoshi K., Yamada T., Terato H., Ohyama Y., Monden Y., Arai T., Nishimura S., Aburatani H., Lindahl T., Ide H., Distinct repair activities of human 7,8-dihydro-8-oxoguanine DNA glycosylase and formamidopyrimidine DNA glycosylase for formamidopyrimidine and 7,8-dihydro-8-oxoguanine, *J. Biol. Chem.* **275** (2000) 4956-4964.

Asagoshi K., Yamada T., Okada Y., Terato H., Ohyama Y., Seki S., Ide H., Recognition of formamidopyrimidine by *Escherichia coli* and mammalian thymine glycol glycosylases, *J. Biol. Chem.* **275** (2000) 24781-24786.

Bai M., Zhang Z., Xue X., Yang X., Hua L., Fan D., Killing effects of hydroxyl radical on algae and bacteria in ship's ballast water and on their cell morphology, *Plasma Chem. Plasma Process* **30** (2010) 831-340.

Benz R., Zimmermann U., Pulse-length dependence of the electrical breakdown in lipid bilayer membranes, *Biochim. Biophys. Acta* **597** (1980) 637-642.

Boiteux S., O' Connor T.R., Lederer F., Gouyette A., Laval J., Homogeneous *Escherichia coli* Fpg protein, *J. Biol. Chem.* **265** (1990) 3916-3922.

Boiteux S., Gajewski E., Laval J., Dizdaroglu M., Substrate specificity of the *Escherichia coli* Fpg protein (formamidopyrimidine-DNA glycosylase): excision of purine lesions in DNA produced by ionizing radiation or photosensitization, *Biochemistry* **31** (1992) 106-110.

Braun J.E., Wanamarta A.H., Westmijze E.J., Wientjes N.M., Wijker C.A., Lafleur M.V., Retèl J., Influence of nucleotide excision repair of *Escherichia coli* on radiation-induced mutagenesis of double-stranded M13 DNA, *Mutat. Res.* **384** (1997) 45-53.

Cadet J., Douki T., Ravanat J.L., Oxidatively generated base damage to

cellular DNA, *Free Radic. Biol. Med.* **49** (2010) 9-21.

Chen C.W., Lee H.M., Chang M.B., Inactivation of aquatic microorganisms by low-frequency AC discharges, *IEEE Trans. Plasma Sci.* **36** (2008) 215-219.

Chetsanga C.J., Lindahl T., Release of 7-methylguanine residues whose imidazole rings have been opened from damaged DNA by a DNA glycosylase from *Escherichia coli*, *Nucleic Acids Res.* **6** (1979) 3673-3684.

Chetsanga C.J., Lozon M., Makaroff C., Savage L., Purification and characterization of *Escherichia coli* formamidopyrimidine-DNA glycosylase that excises damaged 7-methylguanine from deoxyribonucleic acid, *Biochemistry* **20** (1981) 5201-5207.

Dev S.B., Rabussay D.P., Widera G., Hofmann G.A., Medical applications of electroporation, *IEEE Trans. Plasma Sci.* **28** (2000) 206-223.

Feig D.I., Sowers L.C., Loeb L.A., Reverse chemical mutagenesis: identification of the mutagenic lesions resulting from reactive oxygen species-mediated damage to DNA, *Proc. Natl. Acad. Sci. USA* **91** (1994) 6609-6613.

Gogate P.R., Pandit A.B., Engineering design methods for cavitation

reactors II: hydrodynamic cavitation, *AIChE Journal* **46** (2004) 1641-1649.

Gorman A.A., Lovering G., Rodgers M.A.J., The photosensitized formation and reaction of singlet oxygen, O_2*($^1\Delta$), in aqueous micellar systems, *Photochem. Photobiol.* **23** (1976) 399-403.

Gulston M., Fulford J., Jenner T., De Lara C., O'Neill P., Clustered DNA damage induced by γ radiation in human fibroblasts (HF19), hamster (V79-4) cells and plasmid DNA is revealed as Fpg and Nth sensitive sites, *Nucleic Acids Res.* **30** (2002) 3464-3472.

Gupta S.B., Bluhm H., Pulsed underwater corona discharges as a source of strong oxidants: *OH and H2O2, *Water Sci. Technol.* **55** (2007) 7-12.

Hall E.J., Giaccia A.J., Radiobiology for the radiologist, 7th edition (2012) Lippincott Williams and Wilkins, Philadelphia, PA, United States of America.

Hamilton W.A., Sale A.J.H., Effects of high electric fields on microorganisms II. Mechanism of action of the lethal effect, *Biochim. Biophys. Acta.* **148** (1967) 789-800.

Haraguchi K., Greenberg M.M., Synthesis of oligonucleotides containing fapy dG (*N6*-(2-deoxy-α,β-D-*erythro*-pentofuranosyl)-2,6-diamino-4-

hydroxy-5-formamidopyrimidine), *J. Am. Chem. Soc.* **123** (2001) 8636-8637.

Hartman P.S., Eisenstark A., Synergistic killing of *Escherichia coli* by near-UV radiation and hydrogen peroxide: distinction between *recA*-repairable and *recA*-nonrepairable damage, *J. Bacteriol.* **133** (1978) 769-774.

Hatahet Z., Purmal A.A., Wallace S.S., A novel method for site specific introduction of single model oxidative DNA lesions into oligodeoxyribonucleotides, *Nucleic Acids Res.* **21** (1993) 1563-1568.

Hatahet Z., Kow Y.W., Purmal A.A., Cunningham R.P., Wallace S.S., New substrates for old enzymes, *J. Biol. Chem.* **269** (1994) 18814-18820.

Hoebee B., Brouwer J., van de Putte P., Loman H., Retèl J., ^{60}Co γ-rays induce predominantly C/G to G/C transversions in double-stranded M13 DNA, *Nucleic Acids Res.* **16** (1988) 8147-8156.

Ihara S., Water treatment equipment, November 2011, Japan Patent 4813443 B2.

Jiang B., Zheng J., Qiu S., Wu M., Zhang Q., Yan Z., Wue Q., Review on electrical discharge plasma technology for wastewater remediation, *Chem.*

Eng. J. **236** (2014) 348-368.

Jyoti K.K., Pandit A.B., Water disinfection by acoustic and hydrodynamic cavitation, *Biochem. Eng. J.* **7** (2001) 201-212.

Kadowaki K., Sone T., Kamikozawa T., Takasu H., Suzuki S., Effect of water-surface discharge on the inactivation of *Bacillus subtilis* due to protein lysis and DNA damage, *Biosci. Biotechnol. Biochem.* **73** (2009) 1978-1983.

Kasai H., Nishimura S., Hydroxylation of deoxyguanosine at the C-8 position by ascorbic acid and other reducing agents, *Nucleic Acids Res.* **12** (1984) 2137-2145.

Kruszewski M., Iwanenko T., Labile iron pool correlates with iron content in the nucleus and the formation of oxidative DNA damage in mouse lymphoma L5178Y cell lines, *Acta Biochim. Pol.* **50** (2003) 211-215.

Kuda T., Shimizu K., Yano T., Comparison of rapid and simple colorimetric microplate assays as an index of bacterial count, *Food Control* **15** (2004) 421-425.

Kuipers G.K., Poldervaart H.A., Slotman B.J., Lafleur M.V., The influence of formamidopyrimidine-DNA glycosylase on the spontaneous and

γ-radiation-induced mutation spectrum of the *lacZα* gene, *Mutat. Res.* **435** (1999) 141-150.

Leverone M.R., Owen T.C., Tieder F.S., Stewart G.J., Lim D.V., Resting-cell dehydrogenase assay measuring a novel water-soluble formation detects catabolic differences among cells, *J. Microbiol. Methods* **25** (1996) 49-55.

Michaels M.L., Pham L., Cruz C., Miller J.H., MutM, a protein that prevents G · C → T · A transversions, is formamidopyrimidine-DNA glycosylase, *Nucleic Acids Res.* **19** (1991) 3629-3632.

Miichi T., Hayashi N., Ihara S., Satoh S., Yamabe C., Generation of radicals using discharge inside bubbles in water for water treatment, *Rep. Fac. Sci. Engrg. Saga Univ.* **31** (2002) 471-477.

Moreau M., Non-thermal plasma technologies: New tools for bio-decontamination, *Biotechnol. Advances* **26** (2008) 610-617.

Nakano T., Morishita S., Katafuchi A., Matsubara M., Horikawa Y., Terato H., Salem A.M.H., Izumi S., Pack S.P., Makino K., Ide H., Nucleotide excision repair and homologous recombination systems commit differentially to the repair of DNA-protein crosslinks, *Mol. Cell* **28** (2007) 147-158.

O'Brien P.J., Little C., Intracellular mechanisms for the decomposition of a lipid peroxide, I. Decomposition of a lipid peroxide by metal ions, heme compounds, and nucleophiles, *Can. J. Biochem.* **47** (1969) 493-499.

O'Connor T.R., Laval J., Physical association of the 2,6-diamino-4-hydroxy-5*N*-formamidopyrimidine-DNA glycosylase of *Escherichia coli* and an activity nicking DNA at apurinic/apyrimidinic sites, *Proc. Natl. Acad. Sci. USA* **86** (1989) 5222-5226.

Patro J.N., Wiederholt C.J., Jiang Y.L., Delaney J.C., Essigmann J.M., Greenberg M.M., Studies on the replication of the ring opened formamidopyrimidine, FapydG in *Escherichia coli*, *Biochemistry* **46** (2007) 10202-10212.

Pouget J.P., Frelon S., Ravanat J.L., Testard I., Odin F., Cadet J., Formation of modified DNA bases in cells exposed either to Gamma radiation or to high-LET particles, *Radiat. Res.* **157** (2002) 589-595.

Preis S., Klauson D., Gregor A., Potential of electric discharge plasma methods in abatement of volatile organic compounds originating from the food industry, *J. Environ. Manage.* **114** (2013) 125-138.

Rasband W.S., ImageJ, U. S. National Institutes of Health, Bethesda,

Maryland, USA. http://rsb.info.nih.gov/ij/1997-2009 (Accessed January 13, 2012).

Rivière J., Ravanat J.L., Wagner J.R., Ascorbate and H_2O_2 induced oxidative DNA damage in Jurkat cells, *Free Radic. Biol. Med.* **40** (2006) 2071-2079.

Roots R., Okada S., Estimation of life times and diffusion distances of radicals involved in X-ray-induced DNA strand breaks or killing of mammalian cells, *Radiat. Res.* **64** (1975) 306-320.

Sahni M., Locke B.R., The effects of reaction conditions on liquid-phase hydroxyl radical production in gas-liquid pulsed-electrical-discharge reactors, *Plasma Process. Polym.* **3** (2006) 668-681.

Sale A.J.H., Hamilton W.A., Effects of high electric fields on microorganisms, *Biochim. Biophys. Acta Gen. Subj.* **148** (1967) 781-788.

Santos M.E., Drake J.W., Rates of spontaneous mutation in bacteriophage T4 are independent of host fidelity determinants, *Genetics* **138** (1994) 553-564.

Sato M., Ohgiyama T., Clements J.S., Formation of chemical species and their effects on microorganisms using a pulsed high-voltage discharge in

water, *IEEE Trans. Ind. Appl.* **32** (1996) 106-112.

Sato M., Degradation of organic contaminants in water by plasma, *Int. J. Plasma Environ. Sci. Technol.* **3** (2009) 8-14.

Shih K.Y., Locke B.R., Effects of electrode protrusion length, pre-existing bubbles, solution conductivity and temperature, on liquid phase pulsed electrical discharge, *Plasma Process. Polym.* **6** (2009) 729-740.

Soyama H., Muraoka T., Chemical reactor using radical induced by a cavitating jet, *20th International Conference on Water Jetting*, (2010) 259-267.

Su X., Huang Q., Dang B., Wang X., Yu Z., Spectroscopic assessment of argon gas discharge induced radiolysis of aqueous adenine and thymine, *Radiat. Phys. Chem.* **80** (2011) 1343-1351.

Sun B., Sato M., Clements J.S., Optical study of active species produced by a pulsed streamer corona discharge in water, *J. Electrostat.* **39** (1997) 189-202.

Sun B., Sato M., Clements J.S., Use of a pulsed high-voltage discharge for removal of organic compounds in aqueous solution, *J. Phys. D: Appl. Phys.* **32** (1999) 1908-1915.

Takemoto T., Zhang Q.M., Matsumoto Y., Mito S., Izumi T., Ikehata H., Yonei S., 3'-Blocking damage of DNA as a mutagenic lesion caused by hydrogen peroxide in *Escherichia coli*, *J. Radiat. Res.* **39** (1998) 137-144.

Tajiri T., Maki H., Sekiguchi M., Functional cooperation of MutT, MutM and MutY proteins in preventing mutations caused by spontaneous oxidation of guanine nucleotide in *Escherichia coli*, *Mutat. Res.* **336** (1995) 257-267.

Tamaoku K., Ueno K., Akiura K., Ohkura Y., New water-soluble hydrogen donors for the enzymatic photometric determination of hydrogen peroxide. II. *N*-ethyl-*N*-(2-hydroxy-3-sulfopropyl)aniline derivatives, *Chem. Pharm. Bull.* **30** (1982) 2492-2497.

Tchou J., Kasai H., Shibutani S., Chang M.H., Laval J., 8-Oxoguanine (8-hydroxyguanine) DNA glycosylase and its substrate specificity, *Proc. Natl. Acad. Sci. USA* **88** (1991) 4690-4694.

Tchou J., Bodepudi V., Shibutani S., Antoshechkin I., Miller J., Grollman A.P., Johnson F., Substrate specificity of Fpg protein, *J. Biol. Chem.* **269** (1994) 15318-15324.

Terato H., Tanaka R., Nakaarai Y., Nohara T., Doi Y., Iwai S., Hirayama R.,

Furusawa Y., Ide H., Quantitative analysis of isolated and clustered DNA damage induced by Gamma-rays, carbon ion beams, and iron ion beams, *J. Radiat. Res.* **49** (2008) 133-146.

Test S.T., Weiss S.J., Quantitative and temporal characterization of the extracellular H_2O_2 pool generated by human neutrophils, *J. Biol. Chem.* **259** (1984) 399-405.

Toyooka T., Ibuki Y., Takabayashi F., Goto R., Coexposure to benzo[α]pyrene and UVA induces DNA damage: First proof of double-strand breaks in a cell-free system, *Environ. Mol. Mutagen.* **47** (2006) 38-47.

Yasuoka K., Sato K., Development of repetitive pulsed plasmas in gas bubbles for water treatment, *Int. J. Environ. Sci. Tech.* **3** (2009) 22-27.

Yukawa O., Nakazawa T., Radiation-induced lipid peroxidation and membrane-bound enzymes in liver microsomes, *Int. J. Radiat. Biol. Relat. Stud. Phys. Chem. Med.* **37** (1980) 621-631.

Wagner J.R., Hu C.C., Ames B.N., Endogenous oxidative damage of deoxycytidine in DNA, *Proc. Natl. Acad. Sci. USA* **89** (1992) 3380-3384.

Wagner J.R., Cadet J., Oxidation reactions of cytosine DNA compounds by

hydroxyl radical and one-electron oxidants in aerated aqueous solutions, *Acc. Chem. Res.* **43** (2010) 564-571.

Walling C., Fenton's reagent revisited, *Acc. Chem. Res.* **8** (1975) 125-131.

Weiss S.J., Neutrophil-mediated methemoglobin formation in the erythrocyte. The role of superoxide and hydrogen peroxide, *J. Biol. Chem.* **257** (1982) 2947-2953.

Wiederholt C.J., Delaney M.O., Pope M.A., David S.S., Greenberg M.M., Repair of DNA containing FapydG and its β-C-nucleoside analogue by formamidopyrimidine DNA glycosylase and MutY, *Biochemistry* **42** (2003) 9755-9760.

Zhang Q.M., Role of the *Escherichia coli* and human DNA glycosylases that remove 5-formyluracil from DNA in the prevention of mutations, *J. Radiat. Res.* **42** (2001) 11-19.

Acknowledgements

I deeply thank Dr. Hiroaki Terato, the Associate Professor of Saga University and my mentor, for his continuous support and encouragement during this work. I am also grateful to Dr. Satoshi Ihara and Mr. Hironori Ito for their collaboration in this work. I also thank Mrs. Yuka Shimazaki-Tokuyama, Miss Kanae Mori, Mr. Noriki Kobayashi, and Mrs. Yuka Ikeda for their excellent technical assistances.

公表論文

(1) Quantitative analysis of oxidative DNA damage induced by high-voltage pulsed discharge with cavitation.

Kudo K., Ito H., Ihara S., and Terato H., *J. Electrostat.* **73** (2015) 131-139.

(2) Oxidative DNA damage caused by pulsed discharge with cavitation on the bactericidal function.

Kudo K., Ito H., Ihara S., and Terato H., *J. Phys. D Appl. Phys.* 48 (2015) 365401